

137

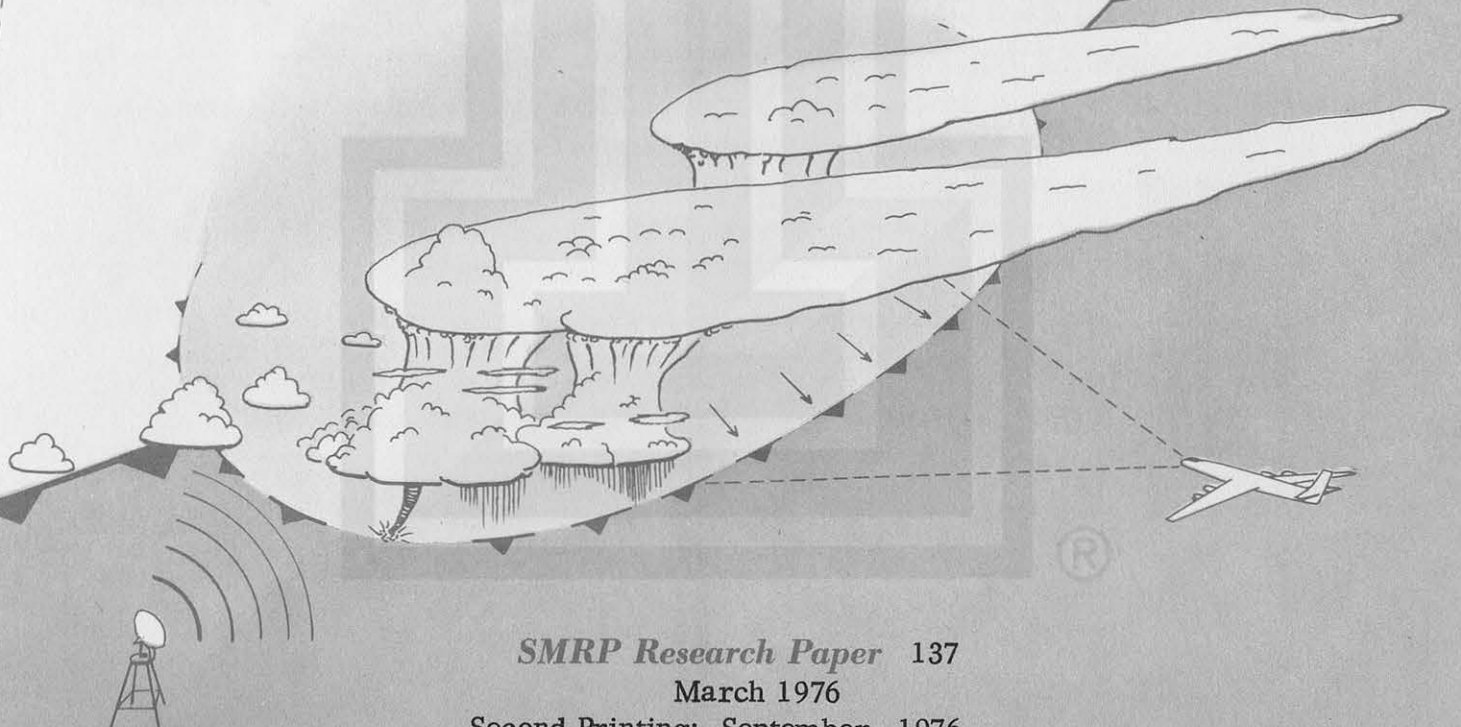
SATELLITE & MESOMETEOROLOGY RESEARCH PROJECT

*Department of the Geophysical Sciences
The University of Chicago*

SPEARHEAD ECHO AND DOWNBURST NEAR THE APPROACH END OF
A JOHN F. KENNEDY AIRPORT RUNWAY, NEW YORK CITY

by

T. Theodore Fujita



SMRP Research Paper 137

March 1976

Second Printing: September, 1976

MESOMETEOROLOGY PROJECT --- RESEARCH PAPERS

- 1.* Report on the Chicago Tornado of March 4, 1961 - Rodger A. Brown and Tetsuya Fujita
- 2.* Index to the NSSP Surface Network - Tetsuya Fujita
- 3.* Outline of a Technique for Precise Rectification of Satellite Cloud Photographs - Tetsuya Fujita
- 4.* Horizontal Structure of Mountain Winds - Henry A. Brown
- 5.* An Investigation of Developmental Processes of the Wake Depression Through Excess Pressure Analysis of Nocturnal Showers - Joseph L. Goldman
- 6.* Precipitation in the 1960 Flagstaff Mesometeorological Network - Kenneth A. Styber
- 7.** On a Method of Single- and Dual-Image Photogrammetry of Panoramic Aerial Photographs - Tetsuya Fujita
8. A Review of Researches on Analytical Mesometeorology - Tetsuya Fujita
- 9.* Meteorological Interpretations of Convective Nephysystems Appearing in TIROS Cloud Photographs - Tetsuya Fujita, Toshimitsu Ushijima, William A. Hass, and George T. Dellert, Jr.
- 10.* Study of the Development of Prefrontal Squall-Systems Using NSSP Network Data - Joseph L. Goldman
11. Analysis of Selected Aircraft Data from NSSP Operation, 1962 - Tetsuya Fujita
12. Study of a Long Condensation Trail Photographed by TIROS I - Toshimitsu Ushijima
13. A Technique for Precise Analysis of Satellite Data; Volume I - Photogrammetry (Published as MSL Report No. 14) - Tetsuya Fujita
14. Investigation of a Summer Jet Stream Using TIROS and Aerological Data - Kozo Ninomiya
15. Outline of a Theory and Examples for Precise Analysis of Satellite Radiation Data - Tetsuya Fujita
16. Preliminary Result of Analysis of the Cumulonimbus Cloud of April 21, 1961 - Tetsuya Fujita and James Arnold
17. A Technique for Precise Analysis of Satellite Photographs - Tetsuya Fujita
- 18.* Evaluation of Limb Darkening from TIROS III Radiation Data - S.H.H. Larsen, Tetsuya Fujita, and W.L. Fletcher
19. Synoptic Interpretation of TIROS III Measurements of Infrared Radiation - Finn Pedersen and Tetsuya Fujita
- 20.* TIROS III Measurements of Terrestrial Radiation and Reflected and Scattered Solar Radiation - S.H.H. Larsen, Tetsuya Fujita, and W.L. Fletcher
21. On the Low-level Structure of a Squall Line - Henry A. Brown
- 22.* Thunderstorms and the Low-level Jet - William D. Bonner
- 23.* The Mesoanalysis of an Organized Convective System - Henry A. Brown
24. Preliminary Radar and Photogrammetric Study of the Illinois Tornadoes of April 17 and 22, 1963 - Joseph L. Goldman and Tetsuya Fujita
25. Use of TIROS Pictures for Studies of the Internal Structure of Tropical Storms - Tetsuya Fujita with Rectified Pictures from TIROS I Orbit 125, R/O 128 - Toshimitsu Ushijima
26. An Experiment in the Determination of Geostrophic and Isalobaric Winds from NSSP Pressure Data - William Bonner
27. Proposed Mechanism of Hook Echo Formation - Tetsuya Fujita with a Preliminary Mesosynoptic Analysis of Tornado Cyclone Case of May 26, 1963 - Tetsuya Fujita and Robbi Stuhmer
28. The Decaying Stage of Hurricane Anna of July 1961 as Portrayed by TIROS Cloud Photographs and Infrared Radiation from the Top of the Storm - Tetsuya Fujita and James Arnold
29. A Technique for Precise Analysis of Satellite Data, Volume II - Radiation Analysis, Section 6. Fixed-Position Scanning - Tetsuya Fujita
30. Evaluation of Errors in the Graphical Rectification of Satellite Photographs - Tetsuya Fujita
31. Tables of Scan Nadir and Horizontal Angles - William D. Bonner
32. A Simplified Grid Technique for Determining Scan Lines Generated by the TIROS Scanning Radiometer - James E. Arnold
33. A Study of Cumulus Clouds over the Flagstaff Research Network with the Use of U-2 Photographs - Dorothy L. Bradbury and Tetsuya Fujita
34. The Scanning Printer and Its Application to Detailed Analysis of Satellite Radiation Data - Tetsuya Fujita
35. Synoptic Study of Cold Air Outbreak over the Mediterranean using Satellite Photographs and Radiation Data - Aasmund Rabbe and Tetsuya Fujita
36. Accurate Calibration of Doppler Winds for their use in the Computation of Mesoscale Wind Fields - Tetsuya Fujita
37. Proposed Operation of Instrumented Aircraft for Research on Moisture Fronts and Wake Depressions - Tetsuya Fujita and Dorothy L. Bradbury
38. Statistical and Kinematical Properties of the Low-level Jet Stream - William D. Bonner
39. The Illinois Tornadoes of 17 and 22 April 1963 - Joseph L. Goldman
40. Resolution of the Nimbus High Resolution Infrared Radiometer - Tetsuya Fujita and William R. Bandeen
41. On the Determination of the Exchange Coefficients in Convective Clouds - Rodger A. Brown

- * Out of Print
 ** To be published

(Continued on back cover)

SPEARHEAD ECHO AND DOWNBURST NEAR THE APPROACH END OF
A JOHN F. KENNEDY AIRPORT RUNWAY, NEW YORK CITY^{2,3}

by

T. Theodore Fujita¹

TABLE OF CONTENTS

1. INTRODUCTION AND SUMMARY	1
2. SATELLITE DATA	2
3. MESOSCALE WEATHER SITUATION	8
4. SPEARHEAD ECHO	16
5. TIME-SPACE ANALYSIS OF APPROACH AREA	20
6. FLIGHT PATHS IN RELATION TO RADAR ECHOES	29
7. EFFECTS OF DOWNBURST AND WIND SHEAR	33
8. SPECULATION ON SPEARHEAD ECHOES	43
9. CONCLUSIONS	46
Acknowledgements	48
References	49
Glossary of New Terms (Byers and Fujita)	50
Subject Index	51

1. Professor of meteorology and Director of SMRP. Department of the Geophysical Sciences, The University of Chicago, Chicago, Illinois 60637.

2. Satellite meteorological aspects of this research have been sponsored by the National Oceanic and Atmospheric Administration under grant 04-4-158-1 (NESS) and by the National Aeronautics and Space Administration under grant NGR 14-001-008.

Aircraft data were obtained from the National Transportation Safety Board Docket No. SA-451 Exhibits (1975) and analyzed in cooperation with the Flight Safety Department of Eastern Airlines.

3. A copy of this report can be obtained from:

OFFICE OF T. THEODORE FUJITA, Department of the Geophysical Sciences, The University of Chicago, Chicago, Illinois 60637, U. S. A.

or from:

FLIGHT SAFETY DEPARTMENT, MIACK, EASTERN AIRLINES
Miami International Airport, Miami, Florida 33148, U. S. A.

1. INTRODUCTION AND SUMMARY

Fourteen aircraft either attempted to land or landed on runway 22-L of John F. Kennedy International Airport (JFK) during a 25-min period on June 24, 1975. This was between 1944 and 2009 GMT (3:44 and 4:09 PM Local Time) when thunder-showers were in progress in the New York City area.

At 1956 GMT a DC-8 experienced considerable difficulty in landing after encountering a strong crosswind shear near the approach end. The next flight, an L-1011 airplane, abandoned the approach because it was pushed down and drifted to the right during the critical period. Two flights then landed without incident. Finally, a B-727 descended normally on the glideslope down to 400 ft where it encountered heavy rain. The downdraft in the rain was so strong that the aircraft contacted the approach lights, 2,400 ft short of the runway.

Detailed examination of meteorological conditions revealed that the growth rate of the JFK Thunderstorm was at its peak when the accident occurred. The radar echo of the storm appeared as a spearhead moving faster than any other echo in the vicinity. Hidden in the spearhead echo were four to five cells of intense downdrafts which are to be called "downburst cells". Apparently, those aircraft which flew through the cells encountered considerable difficulties in landing, while others landed between the cells without even noticing the danger areas on both sides of the approach path.

Extensive analyses of satellite, radar, and synoptic data were performed, leading to the establishment of a model of the spearhead storm and downburst cells. The responses of aircraft in downburst cells were then examined in detail. This has led to the conclusion that a plane can be seriously affected by crosswind shear, headwind or tailwind shear, and a downburst of air current.

At the present time, there is no way of predicting the occurrence of these phenomena both in time and space. Additional anemometers at and around the major airports and better real time assessment of wind and radar data, coupled with knowledge of these small but violent downbursts, will be of great help in the future for minimizing accidents of this nature.

2. SATELLITE DATA

The life history of the JFK Thunderstorm was depicted by the infrared and visible images of SMS-1, a geostationary satellite positioned above the equator at 75°W longitude. A pair of IR and visible pictures at 30-minute intervals is available.

The satellite imagery closest to 2005 GMT, the accident time, was obtained at about 2003 GMT. Unfortunately, the image had been transmitted with coastlines and state boundaries in dots which cannot be removed from the image. An attempt was made to superimpose the precise coastlines so as to determine the three-dimensional features of the JFK Thunderstorm at the time of the accident (see Figure 1).

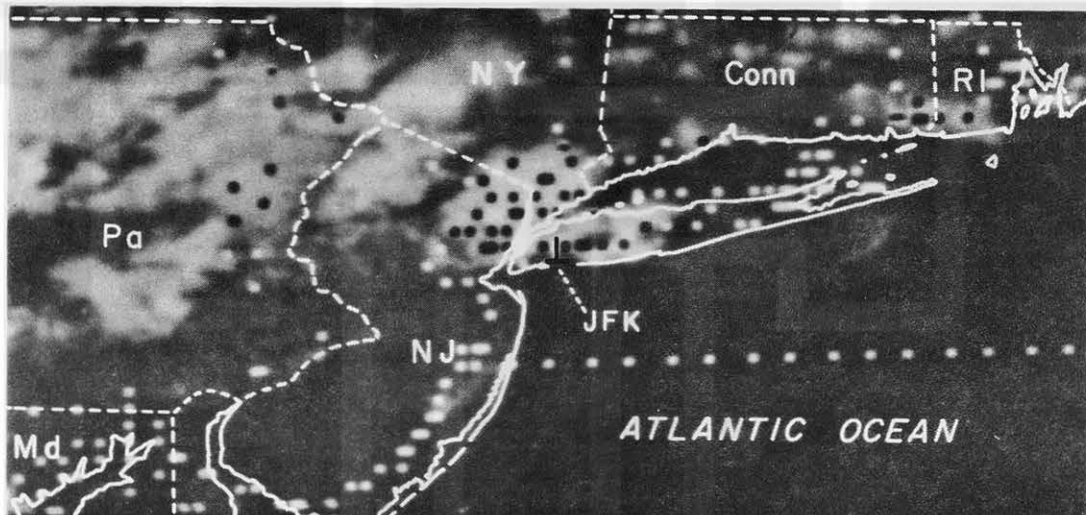


Figure 1. Visible picture of the JFK Thunderstorm at 2003 GMT, about 2 minutes before the aircraft accident. An inverted T symbol is the projected length of a 45,000-ft high, imaginary pole at JFK as seen from the satellite. The image of a cloud at 45,000 ft will shift northward as much as the length of the pole in this figure.

There are two distinct shadows to the east of the anvil clouds spreading out from the storm tops. Another important feature of the storm is an arc cloud extending west to east along the south coast of Long Island through the JFK Airport. Usually an arc cloud expands rapidly out from the storm area. The existence of a sea breeze, however, prevented the southward advance of the arc cloud beyond the JFK Airport (Figure 2).

The height of the anvil cloud to the northeast of JFK was 41,000 ft. The other anvil to the north was 43,000 ft high. These heights were computed from the cloud-

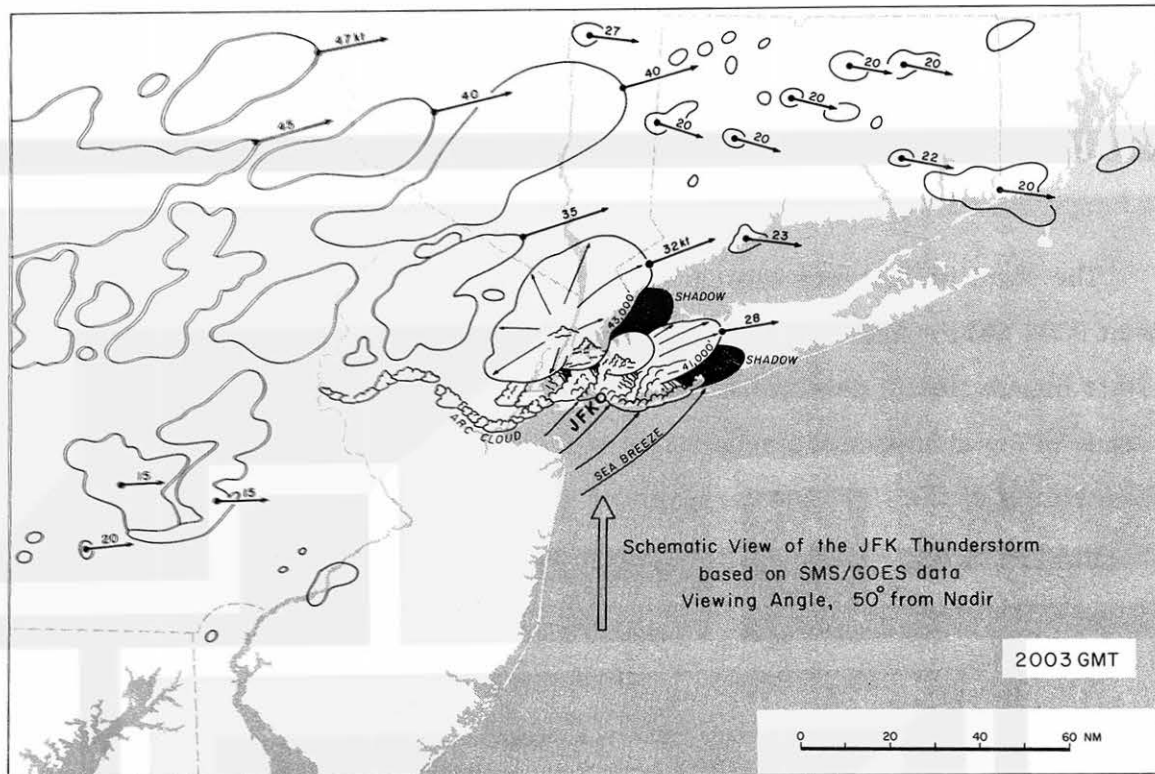


Figure 2. Schematic view of the JFK Thunderstorm drawn on the basis of the geostationary satellite data. The circle identified as JFK is the location of the airport. An arc cloud is seen just to the south of the thunderstorm activity. Its southward advancement is prevented by the sea breeze. The arrowhead vectors denote the cloud motion in knots.

shadow relationship. As indicated by the arrows, the spreading rate of the anvils was about 30 kts toward the east-northeast.

The precursor of the JFK Thunderstorm was the cumulus line A - B seen in northern New Jersey at 1703 GMT (Figure 3). Within 30 minutes, the west end of the cumulus line grew explosively into a towering cumulus (Figure 4). The growth continued to 1803 GMT when the west end, A, became overwhelmingly larger than the east end, B (Figure 5). The visible picture, taken simultaneously, shows a small hole at the center of cloud A.

At 1833 GMT, the north end of cloud A displayed a small bulge (Figure 6). The corresponding visible picture implies that an anvil had already started forming. Within the next 30 minutes the anvil of cloud A grew rapidly (Figure 7).

At 1933 GMT, just about 30 minutes before the accident, a light-grey area appeared inside cloud A. the equivalent blackbody temperature at the boundary of this area was -44°C (Figure 8). The simultaneous visible picture reveals the formation of an arc cloud along the south edge of cloud A.

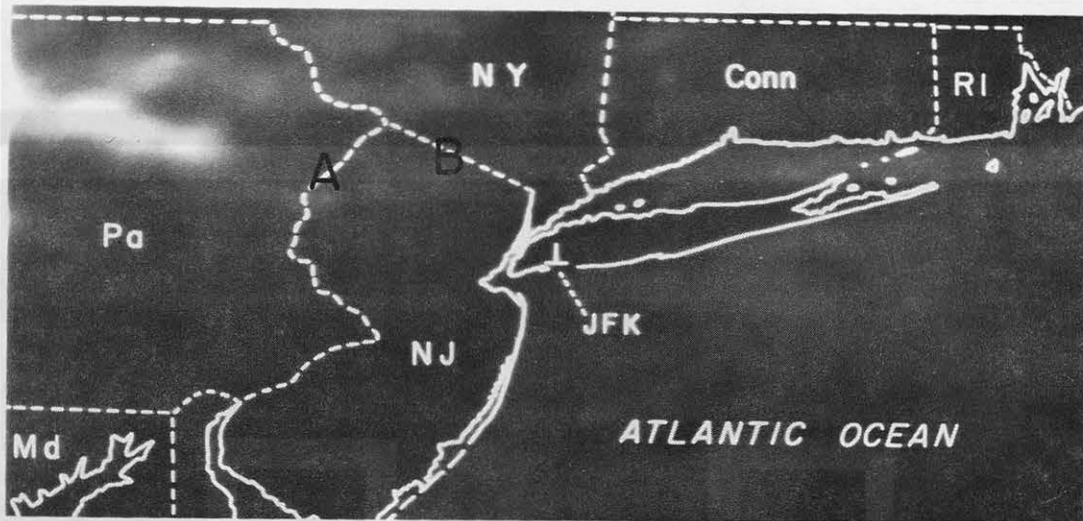


Figure 3. A cumulus line A-B in northern New Jersey. The line was a precursor of the JFK Thunderstorm. Infrared picture at 1703 GMT.

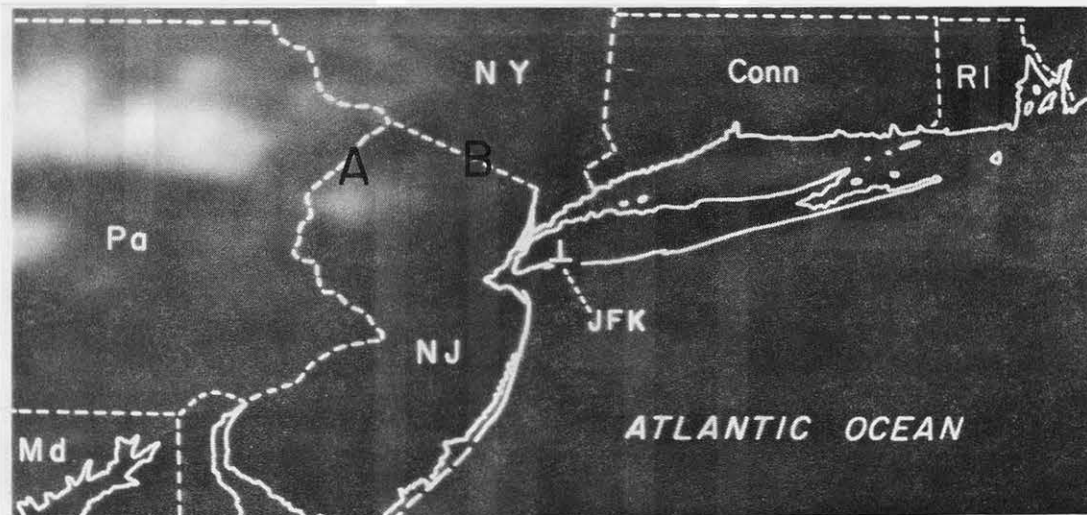


Figure 4. IR picture at 1733 GMT showing an explosive growth of the west end of the cumulus line A-B.

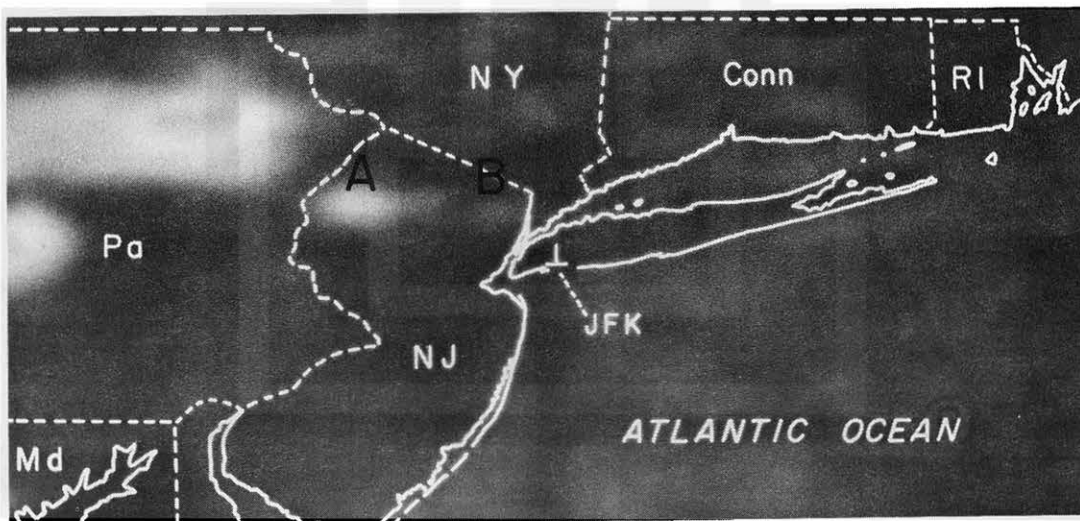


Figure 5. IR picture at 1803 GMT. The west and east ends were separated into clouds A and B.

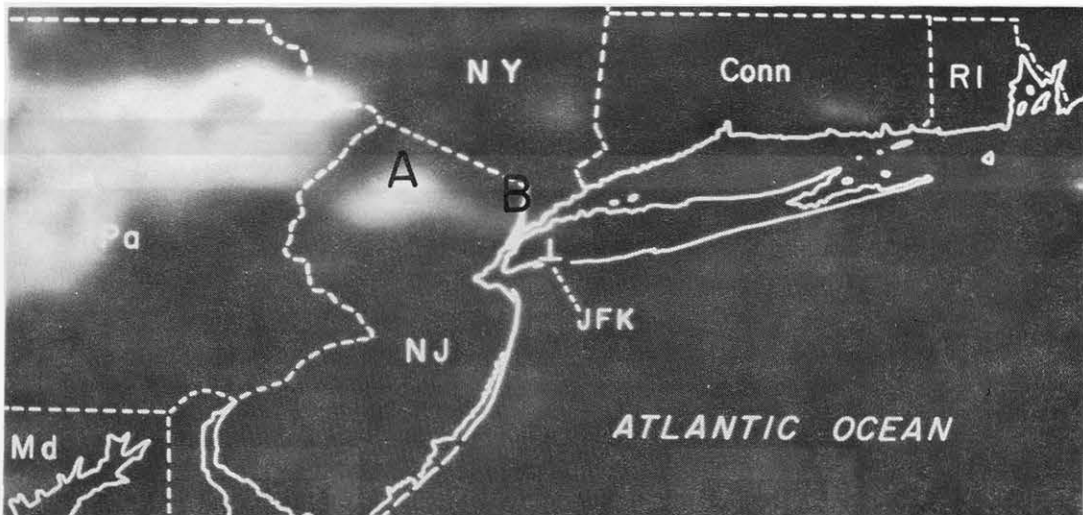


Figure 6. IR picture at 1833 GMT. Cloud B was moving eastward just to the north of JFK. Cloud A started forming an anvil cloud.

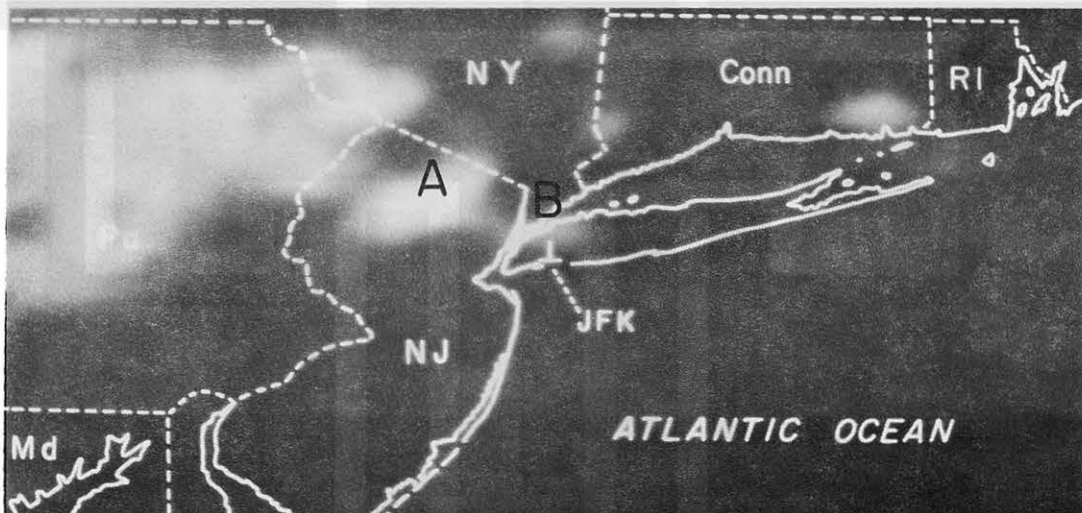


Figure 7. IR picture at 1903 GMT. An anvil is spreading east-north-eastward from cloud A. Cloud B is passing just to the north of JFK.

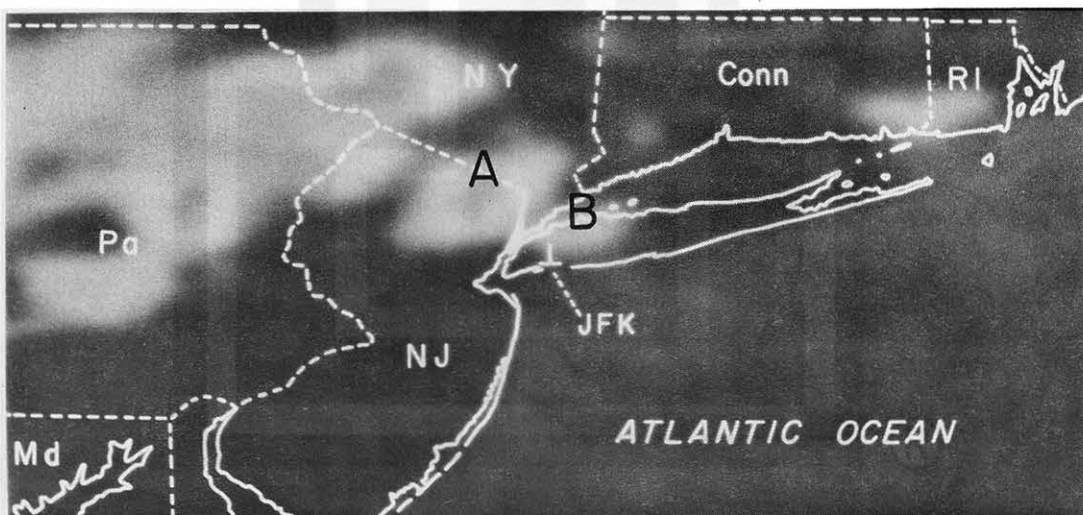


Figure 8. IR picture at 1933 GMT. The first appearance of a dark grey area inside cloud A. The area is characterized by -44°C or colder temperature; correctly, equivalent blackbody temperature.

At 2003 GMT, cloud A and B had joined into a huge thunderstorm complex. Meanwhile, the organization of a long squall line was taking place far to the west of JFK. In many cases, an isolated thunderstorm ahead of a squall line is characterized by severe weather (Figure 9).

A sequence of three pictures taken at 2033 GMT (Figure 10), 2103 GMT (Figure 11), and 2133 GMT (Figure 12) reveals that the areas of overall cloud as well as the areas of cold cloud tops kept increasing.

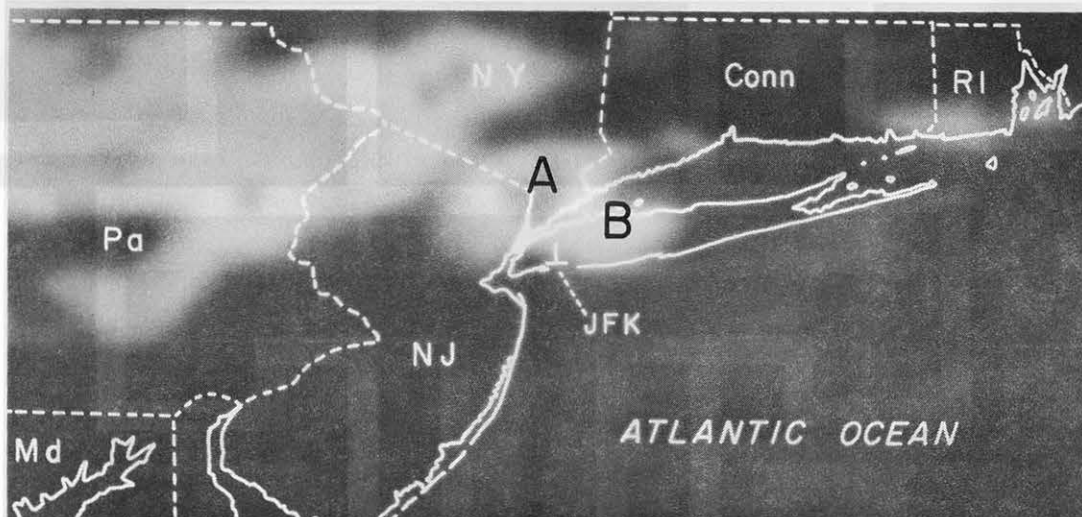


Figure 9. IR picture at 2003 GMT, two minutes before the aircraft accident at JFK. An inverted T denotes the projection of an imaginary, 45,000-ft tower at JFK.

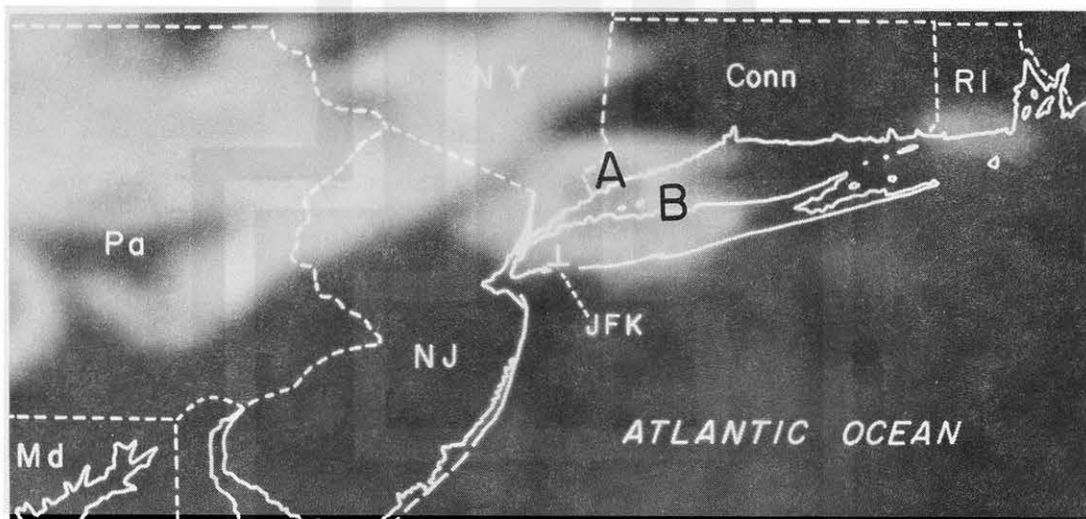


Figure 10. At 2033 GMT, the JFK Thunderstorm became an isolated storm situated ahead of an active squall line.

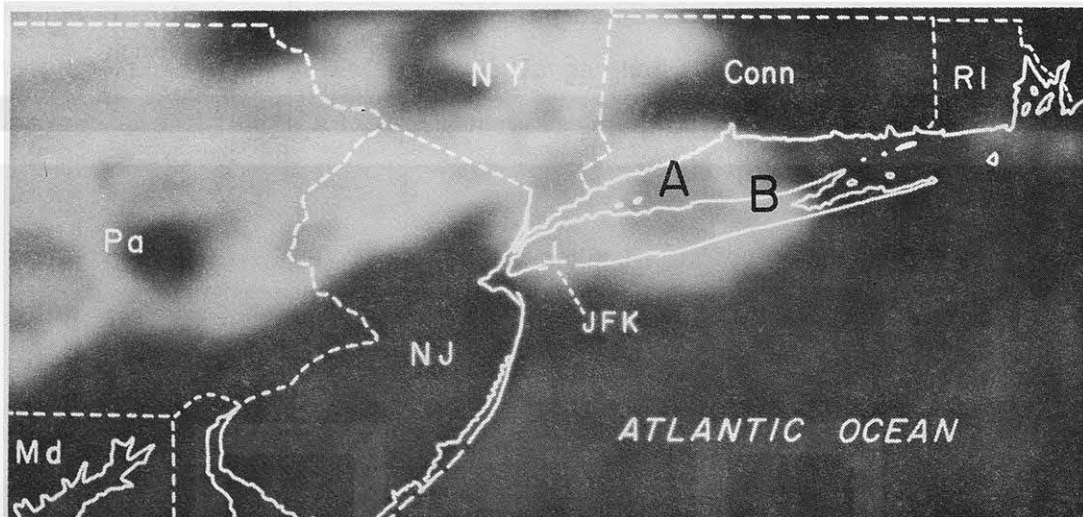


Figure 11. IR picture at 2103 GMT when the growth rate of the JFK Thunderstorm was decreasing.

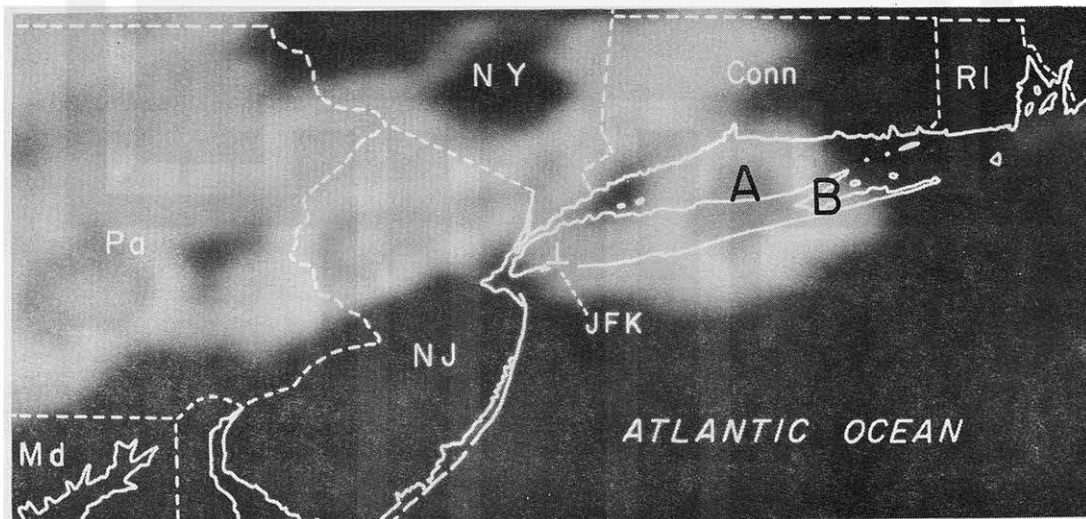


Figure 12. IR picture at 2133 GMT. The cloud area was 3200 sq. nautical miles, while the radar echo covered an area as small as 100 sq. nautical miles. The JFK Thunderstorm is decaying rapidly.

It should be noted, however, that the rate of increase in the cloud area reached its maximum at about 2000 GMT (Figure 13). Likewise, the growth rate of the -44°C area hit the maximum at about the same time. Furthermore, the area of radar echo also reached the peak. Evidently the accident occurred when the JFK Thunderstorm was in its most active stage.

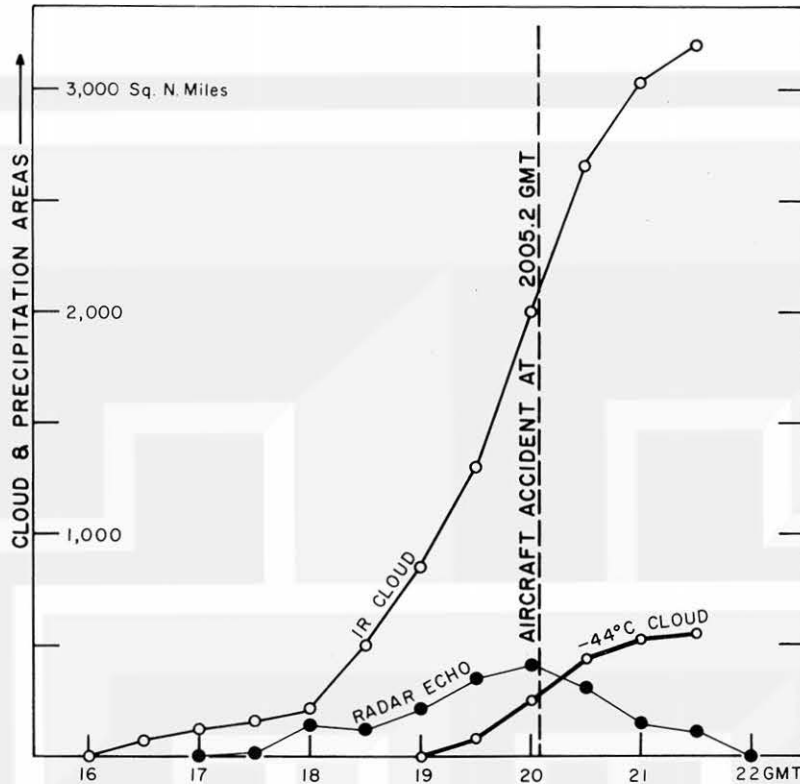


Figure 13. Variation of the cloud imagery and radar-echo areas during a 6-hour period on June 24, 1975. The rates of increase in the cloud and -44°C isotherm areas reached their maxima at about 2005 GMT. At the same time, the radar-echo area hit its peak, suggesting that the accident occurred during the height of the JFK Thunderstorm.

3. MESOSCALE WEATHER SITUATION

Satellite pictures taken during the early afternoon showed that there were scattered shower activities in Pennsylvania. A 300-mile wide band of smog extended toward the east-northeast from Virginia into the Atlantic. Four- to five-mile visibility was reported from JFK, La Guardia (LGA), and Newark (EWR) Airports.

Since the nationwide weather maps are inadequate in examining local storm activities, mesoscale analyses within a 100-mile range from JFK were undertaken. The mesoscale in meteorology is defined as being the scale of motion within 10 to 100 miles in horizontal dimensions. The gross features of most thunderstorms will fall into this scale.

The three major airports serving New York City and vicinity are JFK, LGA, and EWR. JFK is located on the northeast edge of Jamaica Bay, about 2 miles inland from Rockaway Beach on the Atlantic coast of Long Island (Figure 14).

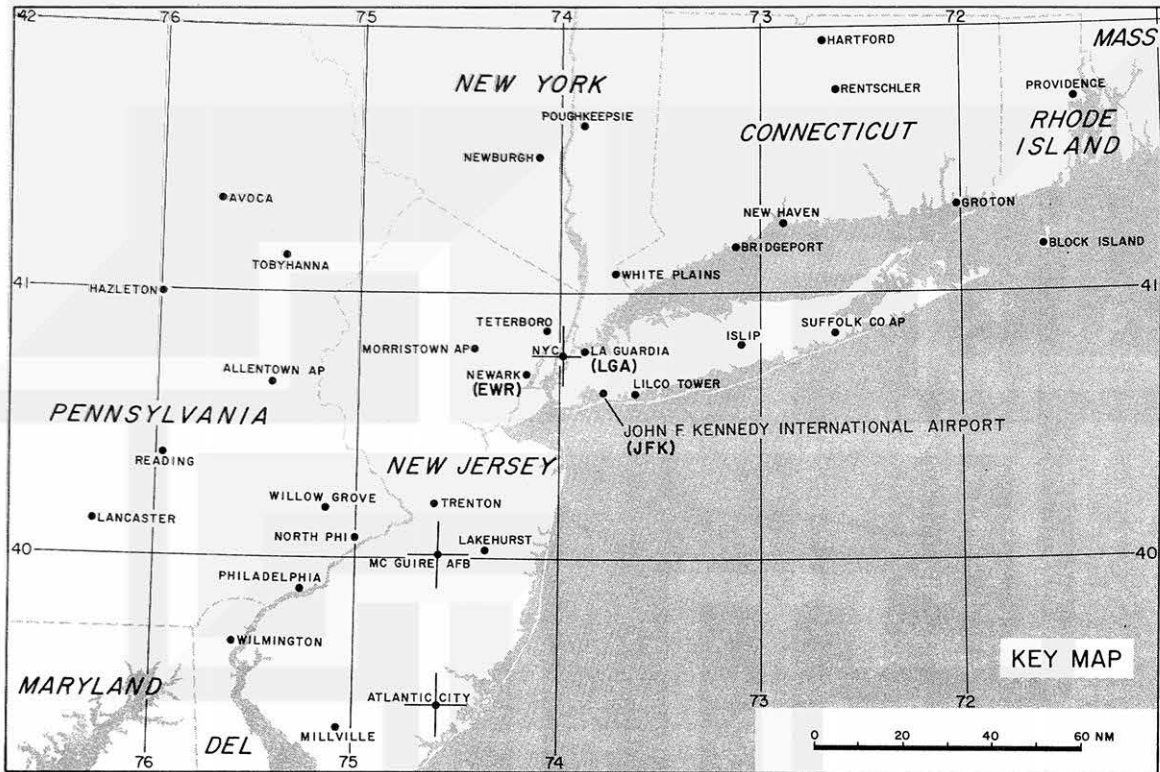


Figure 14. A key map showing the area of the mesoscale weather analyses.

The mesoscale analysis map for 1753 GMT reveals a very complicated thermal structure of a weak front extending from central Pennsylvania to Rhode Island. It is a definite cold front in Pennsylvania and in New Jersey, where it is very hot to the south of the front. The temperature contrast was enhanced by the showers just to the north of the front (Figure 15).

From southern Connecticut to Rhode Island, the temperature gradient was apparently the opposite. It was 90° to 93° F to the north of the front, while the sea breeze temperature to the south was in the 70's or 80's. A line of sea breeze cumuli was seen in southern Connecticut and Rhode Island.

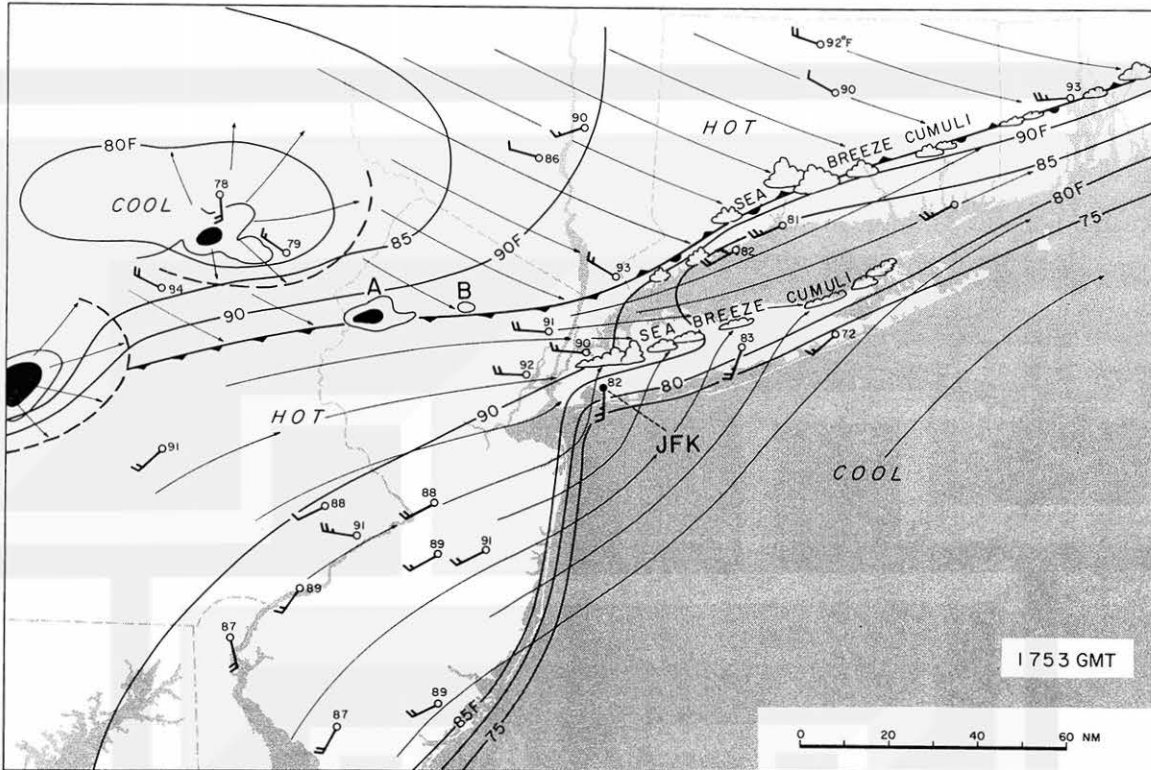


Figure 15. The mesoscale weather situation at 1753 GMT. The numbers by the stations indicate the air temperatures in Fahrenheit. Winds are plotted by doubling the barbs. One full barb denotes 5-kt wind.

Due to solar heating, the Long Island sea breeze was blowing inland across the Atlantic beaches. Apparently there was a weak sea breeze from Long Island Sound, giving rise to the formation of sea-breeze cumuli along the island's north coast. An early stage of the JFK Thunderstorm can be seen in northwestern New Jersey on the cold front. The storm was moving toward the east-southeast at 16 kts. At 1851 GMT it was located on the cold front in north-central New Jersey.

Although the main storm, A, was still on the front, the forerunner, B, moved away from the front and split into two cells--one located over lower Manhattan and the other northeast of LGA (Figure 16). For location of LGA, refer to Figure 14.

Dramatic changes in the echo pattern took place during the one-hour period between 19 and 20 GMT. The JFK Thunderstorm moved very rapidly toward the western tip of Long Island. A line of arc cloud developed along the leading edge of

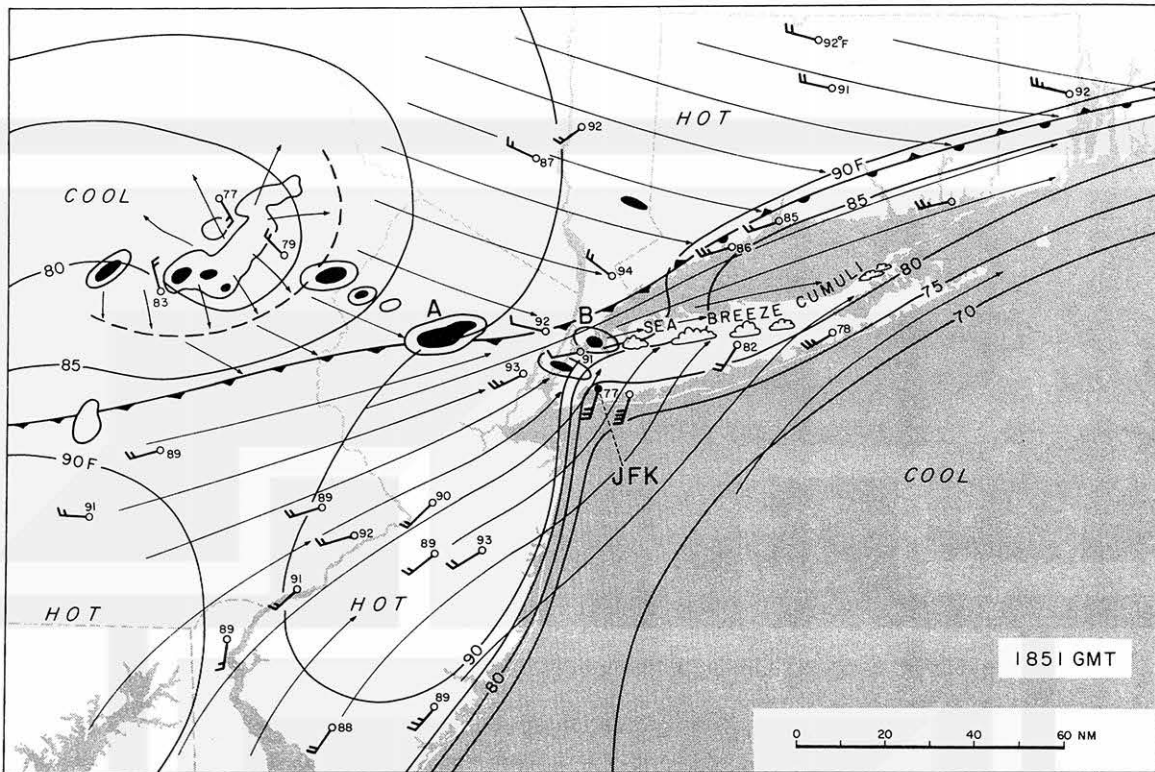


Figure 16. The mesoscale weather situation at 1851 GMT. One full barb denotes 5-kt wind.

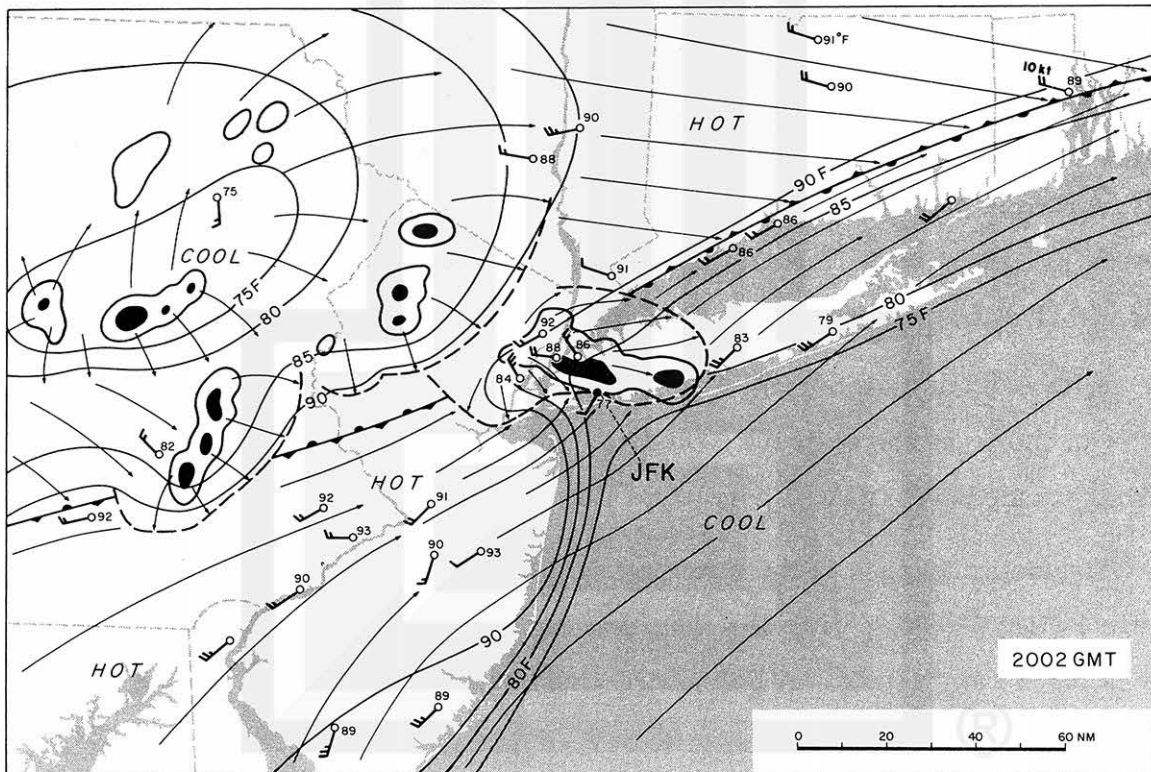


Figure 17. The mesoscale weather situation at 2002 GMT. Aircraft accident occurred at 2005 GMT and the airport was closed. One full barb denotes 5-kt wind.

the overall outflow, the south edge of which was held back by the cold sea breeze from the Atlantic. In fact, the sea-breeze temperature was cooler than that of the thunderstorm outflow. JFK, in the sea breeze, reported a temperature of 77°F while LGA, in the outflow, reported 86°F (Figure 17).

The squall line activity in western Pennsylvania and northern New Jersey was intensifying rapidly. As a result, a surge of northwesterly winds became apparent in advance of a line of echoes.

The mesoscale analysis map at 2053 GMT, about 5 PM, EDT, reveals that the JFK Thunderstorm was weakening and that it was accompanied by a radial outflow of cold air. JFK, located deep inside the outflow, reported a 76°F surface temperature (Figure 18).

An intense squall line was advancing toward central New Jersey where surface temperature was in excess of 90°F.

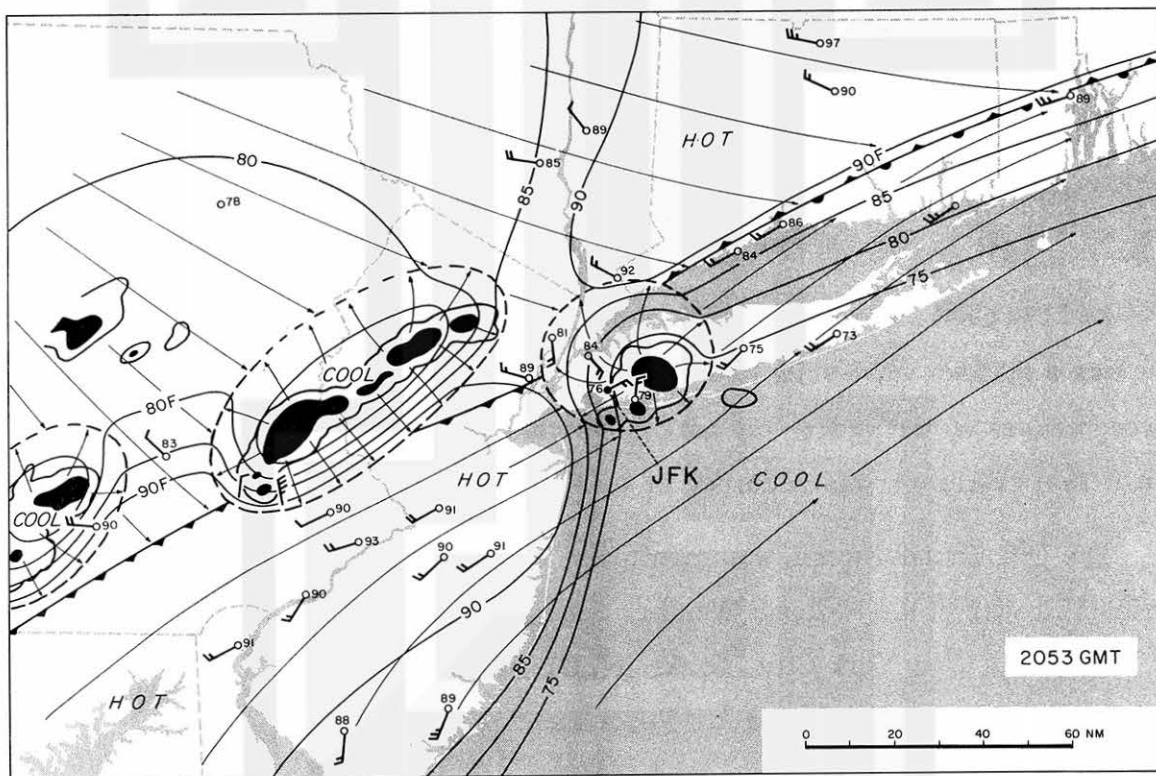


Figure 18. The mesoscale weather situation at 2053 GMT. Runway 13R-31L open for landing at 2053 GMT. One full barb denotes 5-kt wind.

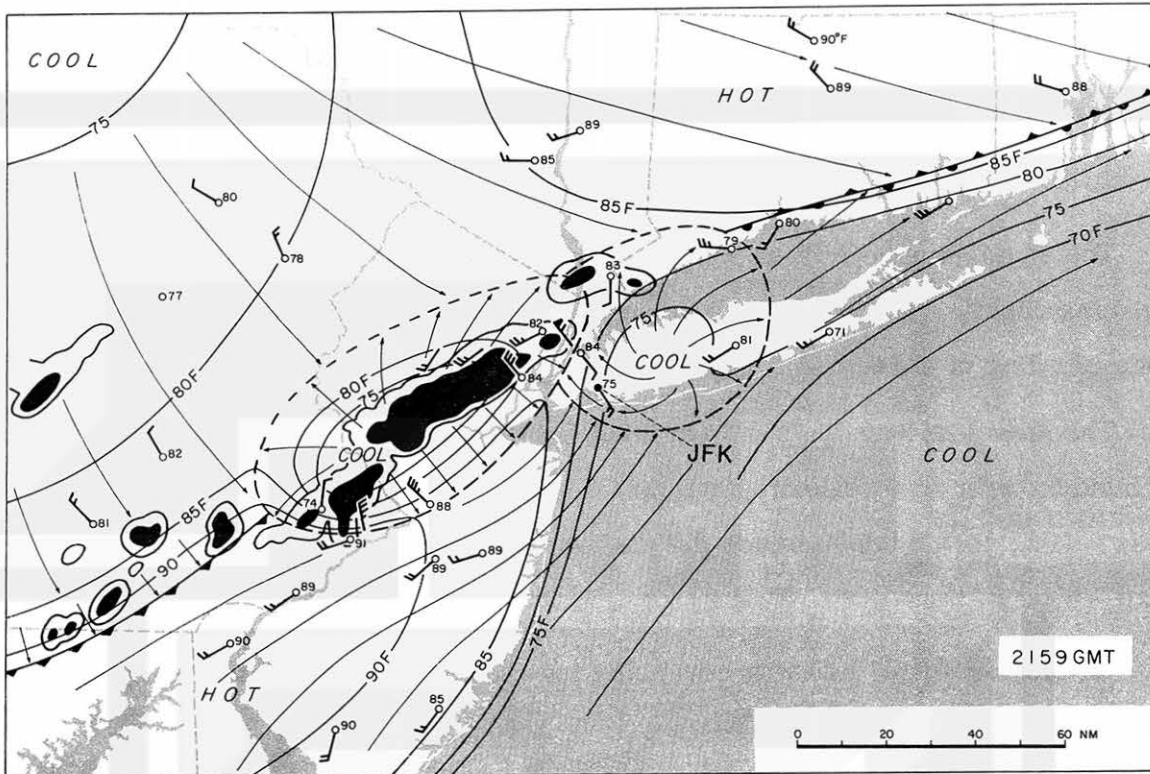


Figure 19. The mesoscale weather situation at 2159 GMT when runway 13L-31R at JFK resumed operations. One barb denotes 5-kt wind.

By 2159 GMT, about 6 PM, EDT, the squall line reached central New Jersey. There was a distinct wind-shift line along its leading edge. In spite of the appearance of strong echoes on the radar, the maximum wind behind the wind-shift line was only 26 kts. This maximum was recorded at LGA at 2207 GMT (Figure 19).

The JFK Thunderstorm was monitored by radar at three stations.

1. WSR-57 radar of the National Weather Service Forecast Office at Rockefeller Center, New York City, N. Y. (NYC)
2. AN/FPS-77 radar of McGuire Air Force Base, N. J. (MCG)
3. WSR-57 radar at Atlantic City, N. J. (ACY)

A total of seven measurements of the echo tops of the JFK Thunderstorm were made by these three stations. The results are as follows:

Time	Direct - Dist	Max Top	Echo Motion	Station
1830 GMT	285 - 40 nm	37,000 ft	290 - 20 kts	NYC
1907	008 - 85	48,000	290 - 30	ACY
1932	011 - 86	53,000	290 - 25	ACY
1933	278 - 19	35,000	- - - -	NYC
1936	018 - 45	44,000	300 - 20	MCG
2032	030 - 85	49,000	290 - 25	ACY
2036	045 - 53	40,000	290 - 25	MCG

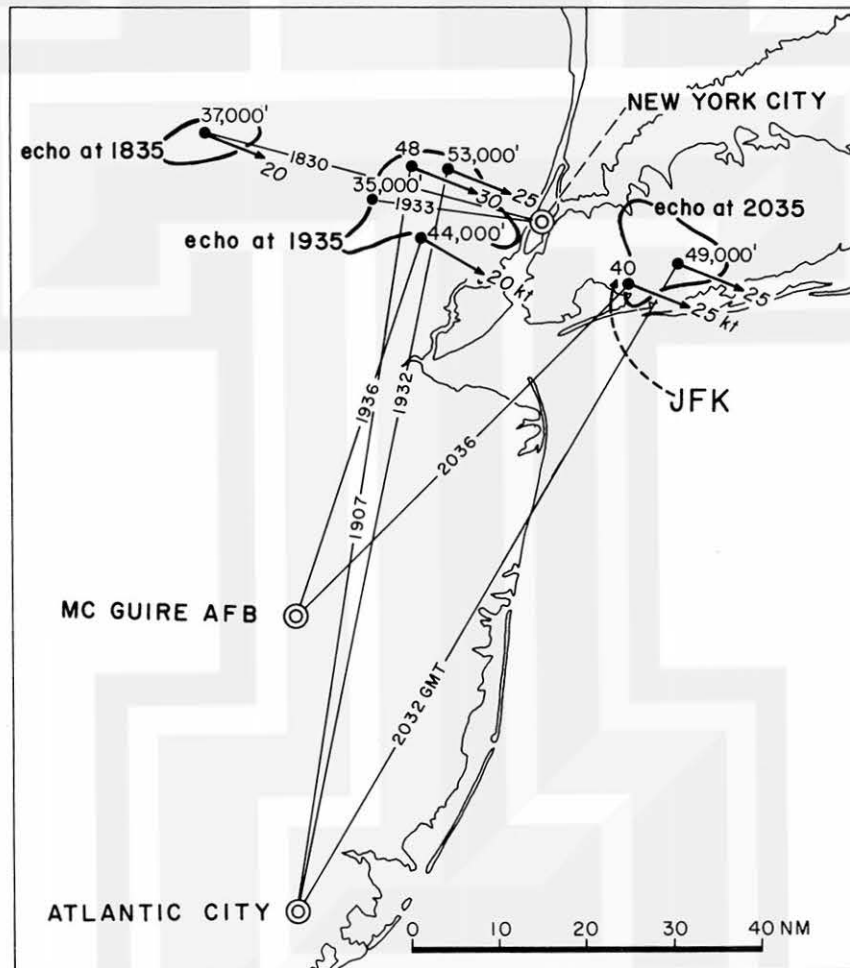


Figure 20. Height of the echo tops of the JFK Thunderstorm measured by three radars: Atlantic City, McGuire Air Force Base, and Rockefeller Center, New York City.

The variation of the echo-top height turned out to be between 35,000 and 49,000 ft. The NYC radar was checked under the direction of Gibson (1975), who found everything to be within the required tolerance.

When these echo-top measurements are plotted on one map, one can see that there are apparent differences in the measured height (Figure 20).

- a. McGuire AFB radar has a tendency to under-estimate the range by 10 to 15%. Range correction would increase the 44,000 to 50,000 ft and the 40,000 to 44,000 ft.
- b. The further the cloud distance from the radar, the higher the echo top. This trend is most significant at about 1935 GMT when all three stations measured the tops within the JFK Thunderstorm area.
- c. It is unlikely that the top of an identical echo was measured simultaneously. There is no way of selecting the identical echo top to be measured by the three radars.
- d. Echo-top height varies rapidly with time. It would be impractical to measure the time and space variations of echo tops by the use of current weather radars.

The satellite pictures, as well as the observations by airline pilots, revealed the existence of an anvil cloud atop the JFK Thunderstorm. The heights of the anvil measured from the shadows were 41,000 and 43,000 ft (see Figure 2). The tropopause was located at about 46,000 ft. Since the tropopause above New York City on June 24, 1975 was not well defined, the spreading of an anvil cloud may have occurred at any height above 40,000 ft where a relatively stable layer existed.

Taking the above evidence and the inevitability of error into consideration, we may assume that the JFK Thunderstorm was topped by anvil clouds at the 40,000 to 43,000-ft level. Since the equivalent blackbody temperature of the anvil was colder than -44°C (air temperature at 36,000 ft) but warmer than -58°C (air temperature at 41,000 ft), its emissivity must have been less than 1.00. The thunderstorm was probably topped by a relatively thin anvil cloud.

The detailed mesoscale weather analyses presented in this section provide a better understanding of the local weather on June 24, 1975. Still, we will have to know why the JFK Thunderstorm was more dangerous than numerous other storms.

4. SPEARHEAD ECHO

Shortly after the aircraft accident, there was speculation that the JFK Thunderstorm had a hook echo in it. A hook echo is known to be extremely dangerous to aviation because it could spawn tornadoes, and all pilots are aware that they should stay clear of hook-echo thunderstorms.

A subsequent examination of radar film from Atlantic City, N. J. by Gibson (1975) disproved the existence of a hook echo. On a visit to the National Weather Service Forecast Office, New York City, in November, 1975, this matter was discussed with him in depth. Neither of us found evidence of a hook echo.

Gibson emphasized a very important characteristic of the JFK Thunderstorm. As he stated in his report, echo A moved to the east-southeast at a speed of 30 to 35 kts, while the forerunner echoes were moving in the same direction at 20 to 25 kts. The greater speed of echo A resulted in an overtaking and subsequent merger of echoes. All of this was taking place in the immediate vicinity of JFK at the approximate time of the aircraft accident.

In order to generalize Gibson's findings, the author made a time-sequence analysis of the JFK Thunderstorm (Figure 21).

It is evident that two forerunner echoes existed to the north and northwest of JFK at 1905 and moved slowly toward the east-southeast. The echo which was moving behind the JFK Thunderstorm also traveled slowly. The motion of these echoes was only 15 to 17 kts. The JFK Thunderstorm, which had been moving rather slowly until 1916 GMT, suddenly accelerated toward JFK. We shall try to determine the reason for this fast movement of the echo.

Within the 11 minutes between 1905 and 1916 GMT, an appendage formed near the east end of the major echo. The first appendage, seen in the 1910.7 GMT picture, was three miles long with a sharp point. The point, somewhat like a spearhead, extended very rapidly. By 1940 GMT, the spearhead appendage became so large that the parent echo began losing its identity. Within a few minutes, the parent echo was drawn quickly into the appendage.

The 1951 GMT radar picture shows that the parent echo was drawn entirely into the appendage, which was moving rapidly toward JFK Airport. The appendage

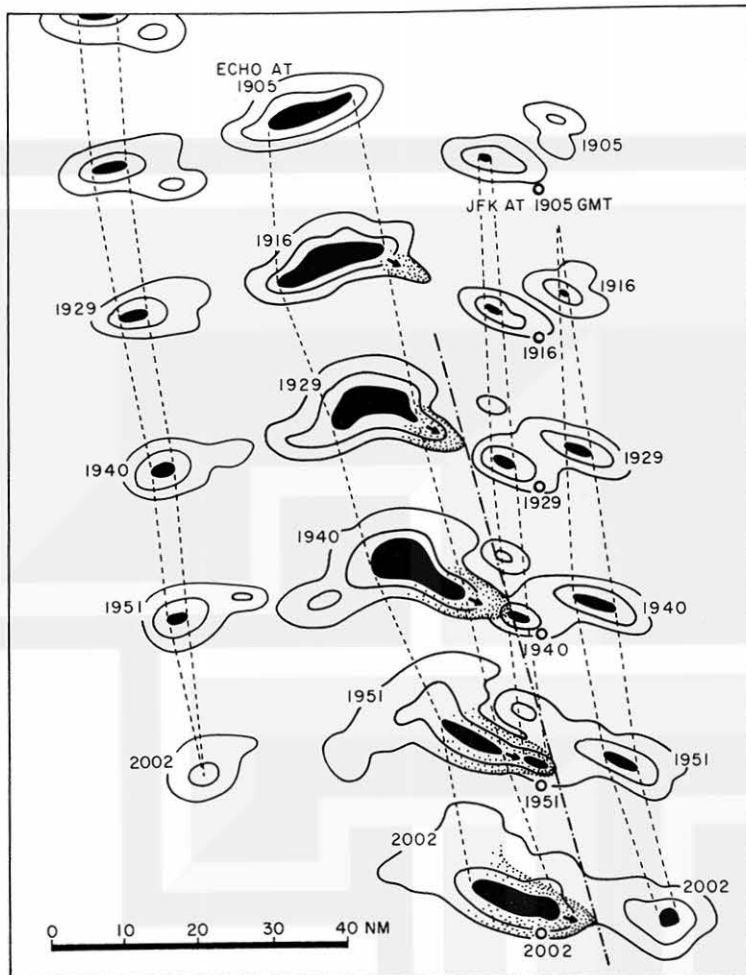


Figure 21. Formation and advance of a spearhead echo. This time sequence shows how a small appendage grew into a spearhead echo, resulting in the decay of the parent echo.

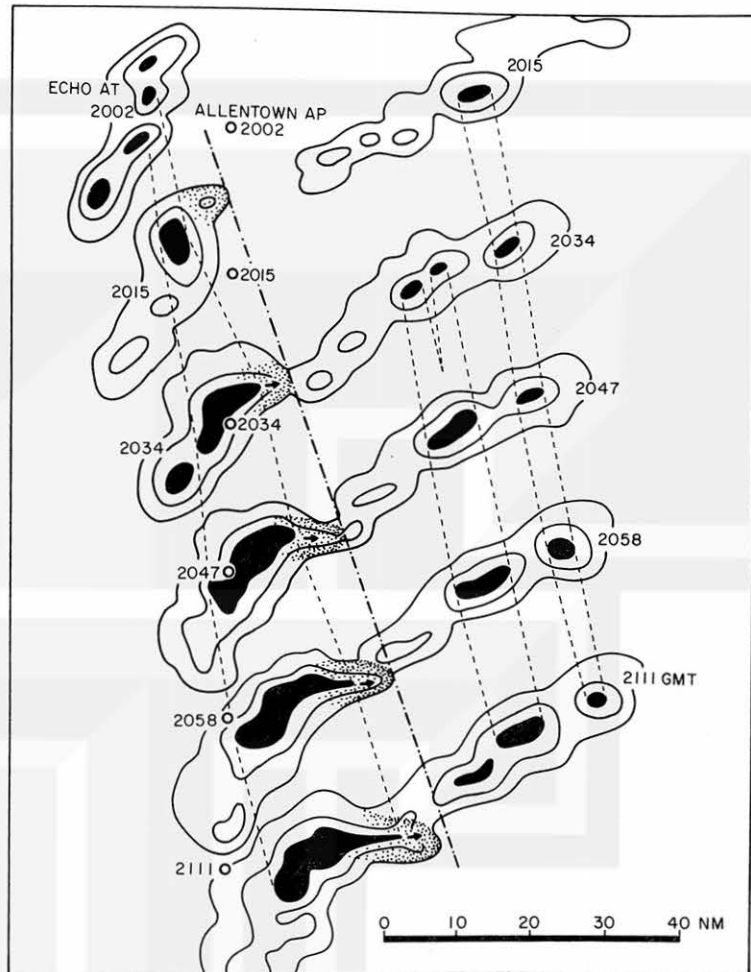
had now lost its identity, redeveloping into a fast-moving "spearhead echo". The spearhead echo merged with a small echo located to the north of JFK Airport at 1951 GMT.

The spearhead echo at 2002 GMT was about 15 miles long and 5 miles wide and located just north of the airport. The radar picture was taken with a 0.2 elevation angle when the JFK Thunderstorm was 80 miles away from the Atlantic City radar. The height of the radar beam above JFK was computed to be about 7,000 ft. Due to the beam width, the image of a point target elongates in the direction perpendicular to the beam. The elongation for a one-degree beam width is 1.3 miles at an 80-mile distance. We must therefore evaluate the radar images of the JFK Thunderstorm, taking these values into consideration.

In view of the suspected relationship between the aircraft accident under investigation and the spearhead echo, we shall define the latter as follows:

SPEARHEAD ECHO: A radar echo with a pointed appendage extending toward the direction of the echo motion. The appendage moves much faster than the parent

Figure 22. Another spearhead echo of June 24, 1975, which developed to the north of Allentown Airport, Pa.



echo which is being drawn in to the appendage. During the mature stage, the appendage turns into a major echo and the parent echo loses its identity. Ground-based weather radar will be able to detect a spearhead echo 100 miles away. It is not known at this time whether airborne radar will be able to detect such a spearhead echo.

In an attempt to determine the frequency of spearhead echoes on June 24, 1975, the Atlantic City radar film was examined in detail, leading to the finding of another spearhead echo. The second one formed just to the north of Allentown in eastern Pennsylvania. At 2015 GMT the echo was about 80 miles from the Atlantic City radar (Figure 22).

The life of a spearhead echo appears to be relatively short. The appendage of the JFK echo started forming at 1910 GMT, reaching its mature stage in about 50 minutes. The Allentown echo repeated a similar cycle between 2015 and 2111 GMT, taking about one hour (Figure 23).

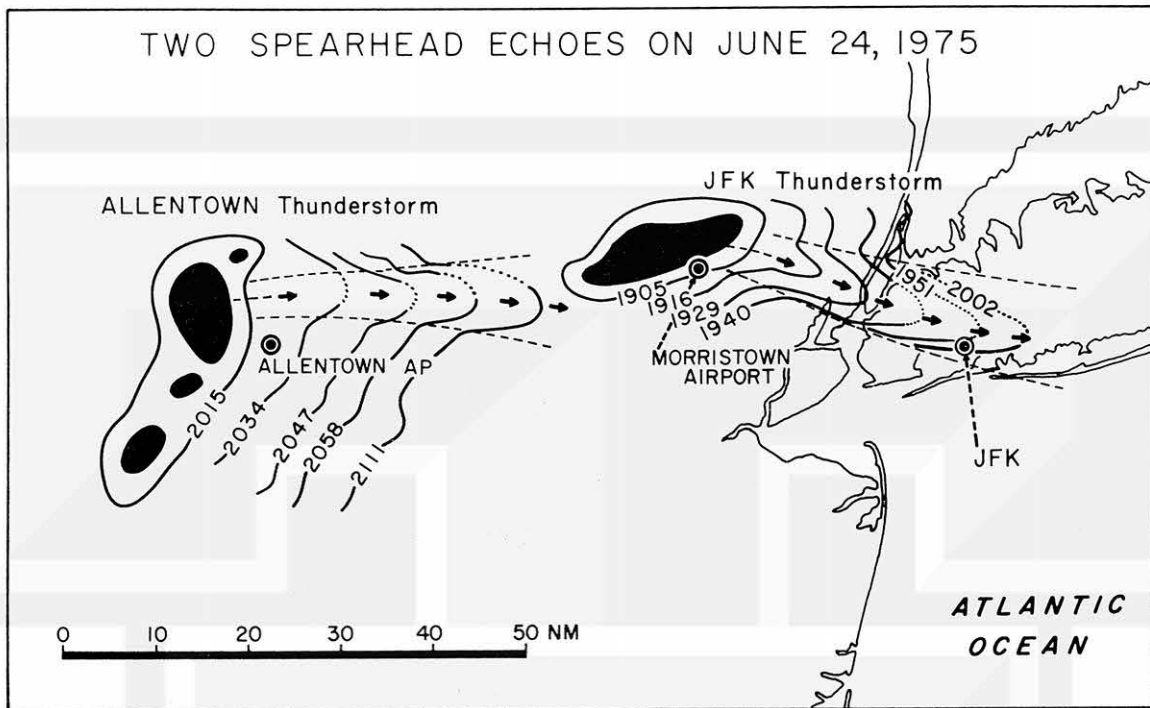


Figure 23. Isochrone of the boundaries of two spearhead echoes, showing their development within approximately one hour.

It was fortunate that Allentown Airfield was not affected by the spearhead echo. On the other hand, an earlier spearhead echo rushed toward the approach end of one of the JFK runways, 22-L. Within 25 minutes, between 1944 and 2009 GMT, 14 aircraft, including three 747s and two L-1011s, either landed or attempted to land at JFK.

To evaluate the probability of occurrence of spearhead echoes on June 24, 1975, the Atlantic City radar was re-evaluated. The hourly counts of echoes over the Atlantic States are summarized in the following table:

Time	Number of Ordinary Echoes	Spearhead Echoes
1652 GMT	1	0
1753	3	0
1850	13	0
1950	14	1
2052	18	1
2152	19	0
2247	24	0
2354	15	0
Total	107	2

This table shows that only 2 out of 109 echoes are classified as spearhead echoes. All others were, more or less, summer-time echoes which may not present serious problems in aviation.

Gibson's (1975) statement is very important in this regard. His record shows that the only report of a wind gust equal to or in excess of 35 kts came from the Morristown, N. J. Municipal Airport, which reported 55 kts occurring at 1915 GMT. Although he does not preclude the possibility of an unreported occurrence, his record was the only report received for June 24, 1975 from northern New Jersey, New York City and Long Island. The Morristown Airport is located 32 miles to the west-north-west of JFK. A spearhead echo was forming just to the north of the airport when the 55-kt wind was reported (Figure 23).

The probability that an airport will be under the influence of a spearhead echo is very low, say less than two percent of the thunderstorm probability. Furthermore, the location of aviation hazards is limited to only a fraction of the spearhead-echo area. This subject will be discussed in the following chapter.

5. TIME-SPACE ANALYSIS OF APPROACH AREA

During the critical period of 22 minutes, prior to the accident at 2005.2 GMT, 12 aircraft made approaches along the localizer-course of the instrument landing system (ILS) of runway 22-L at JFK. However, not all aircraft encountered difficulties serious enough that the pilots reported it to the tower.

The chronological events experienced by the landing aircraft are tabulated.

Aircraft	Type	Landing Time	Approach and Landing Conditions
A	747	* 1944 GMT	Some wind shear; insignificant to report to tower
B	707	* 1946	Add power from 500 ft down; normal touchdown.
C	DC-9	* 1948	Experienced a downdraft before the touchdown in rain.
D	707	1949	Approach and landing were normal.
E	747	1951	Experienced little rain on touchdown.
F	747	* 1952	Some wind shear, not necessary to report to tower.
G	707	* 1954	At 200 ft, 8° drift to the left.
H	DC-8	** 1956	Strong, sustained sink followed by strong crosswind.
I	L-1011	** 1958	Plane sank while drifting right; abandoned approach.
J	DC-8	1959	Landed normally without difficulties.
K	BEECH	* 2002	Applied power to recover from sink; landing normal.
L	727	** 2005	Caught in intense downburst at 400 ft. Accident.
M	727	2007	Abandoned approach due to accident.
N	L-1011	2009	Abandoned approach due to accident.

**experienced major difficulty

*insignificant difficulty

It is important, first of all, to recognize that the landing difficulties occurred during three distinct periods separated by those of normal landings. The three periods were 1945 to 1949, 1952 to 1959, and 2002 to 2005+. If we assume the traveling motion of the spearhead echo to be 30 kts, the horizontal dimension of the hazardous areas would be only 3 to 5 miles. A pilot could complete a normal approach and landing during the calm period without being able to see or being aware of the danger areas on either side of his approach path.

From a meteorological point of view, it is impractical to reconstruct the three-dimensional wind field based on the information of surface winds in the approach area. First of all, there is no wind information except eyewitness accounts. Secondly, we cannot expect to determine the time within an accuracy of one minute or less. It is a very difficult problem to analyze the airflow of small scale disturbances.

To overcome analytical difficulties, the concept of TIME-SPACE COORDINATES was developed. For the original work, refer to Fujita (1963). The coordinates consist of the paths of the aircraft shifted successively in a direction opposite to that of the movement of the spearhead echo. In constructing the time-space coordinates for this investigation, the approach path of runway 22-L at JFK was shifted toward 292° true (304° magnetic) at 30 kts (Figure 24).

The coordinates were designed to include the touchdown time between 1943 and 2010 GMT. The map of the JFK area corresponding to the localizer approach of the accident aircraft was placed in the coordinates. The black circles with the time in GMT denote the one-minute positions of the landing aircraft. The take-off positions of the departing aircraft are shown by open circles.

The heights along the glideslope plane are shown at 100 ft intervals. Actual heights are indicated for those aircraft for which the radar and/or altimeter altitudes were available. As a measure of the crosswind component, the aircraft headings at 10-second intervals were plotted after subtracting the magnetic heading of runway 22-L. Since the overall crosswind component was from the right of the path, most aircraft kept correcting a 1° to 8° drift during the localizer approaches.

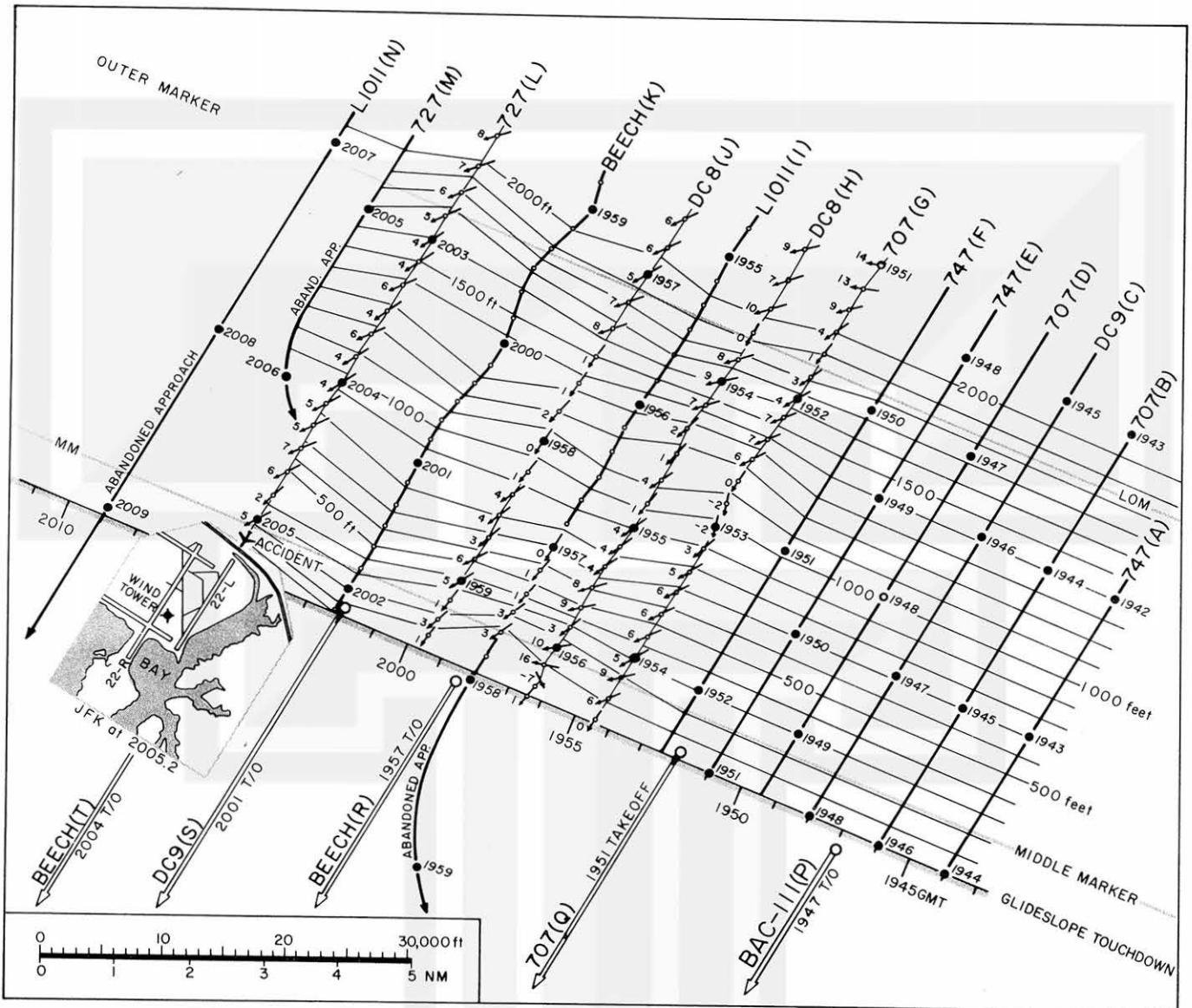


Figure 24. Time-space coordinates of the 22-L approach path relative to the moving weather systems. The glideslope, the outer marker (LOM) and middle marker (MM), and runways were shifted toward 292° true at 30 kts. Aircraft headings at 10-sec intervals were plotted after subtracting the magnetic heading of the runway. The directions of small arrows are exaggerated 5 times.

The airflow patterns near the approach end of 22-L can be depicted by plotting the events experienced by each aircraft. These events are summarized as follows:

Aircraft "A" (747): encountered moderate rain at about the outer marker. There was no turbulence. Broke out into light rain at 1,000 ft. Encountered some wind shear on final approach. It required considerable extra power to maintain approach speed, but the pilot did not consider the wind shear to be significant enough to mention to the tower. (From Exhibit 2-V of the National Transportation Safety Board's (NTSB) Exhibits introduced during a public hearing.)

Aircraft "B" (707): experienced smooth air all the way down to the final approach. The only indication of wind shear or a downdraft was after passing 500 ft. From that point on, the pilot added power to maintain the ILS glideslope and to keep the speed from eroding. Sighted a thunderstorm about a mile to the right of the approach path, just short of runway 22-L at JFK. The rain from the storm was falling on the approach end of the runway. The flight engineer assumed that there was an increased headwind associated with the thunderstorm. (From Exhibit 2-V.)

Aircraft "C" (DC-9): experienced a downdraft at about one mile from the end of runway 22-L. Landed in light rain. (From Exhibit 2-V.)

Aircraft "D" (707): between the outer and middle markers moderate rain was encountered. The approach and landing were normal. The landing roll-out was made on dry runway. (From Exhibit 2-V.)

Aircraft "E" (747): experienced heavy rain at 1,000 ft. There was some wind shear during the early part of the approach. There was little rain on touchdown. (From Exhibit 2-A.)

Aircraft "F" (747): 10 kts headwind and 2° left drift at the outer marker. Entered the rain at about 1,200 ft. Light rain changed into heavy rain. The airborne Inertial Navigation System (INS) indicated a headwind of 15 kts with 4° left drift. Airspeed dropped at 300 ft, requiring power. INS headwind 10 kts with 1° left drift at 100 ft. Rain stopped when over the runway threshold. Landed with 2° left drift. First half of runway was wet and the other half was dry. (From Exhibit 2-V.)

Aircraft "G" (707): encountered extremely heavy rain at about 800 ft. At about 200 ft, drift was 8° left or 18 kts crosswind from right to left of the aircraft. Windshield wipers were operated at high speed in extremely heavy rain. No drift correction required at touchdown in heavy rain. Rolled for about 1,000 ft and broke out on dry runway in sunlight. While on the taxiway, the pilot saw that the next aircraft, "H", was in difficult maneuver. "Thought that the pilot must have been like a cat on a hot tin roof, trying to save his airplane." (From Exhibit 2-V.)

Aircraft "H" (DC-8): encountered strong, sustained downdraft from about 700 ft down to about 200 ft. The pilot used an abnormal amount of power for an unusually long period of time. From 200 ft to touchdown the downdraft was moderate, but the crosswind from the right was very strong. It was blowing about 50 or 55 kts just off the ground, and then all of a sudden there was practically no wind on the ground. The pilot had to use 10° to 15° heading to the right during the ILS approach then it changed to 7° to the left. No drift correction was required at touchdown. (From Exhibits 2-V, 12-B, and Flight Recorder.)

Aircraft "I" (L-1011): everything was normal to about 400 ft. The air was smooth and it was not raining. As the aircraft flew into extremely heavy rain, visibility dropped to zero, and the aircraft started to sink and drift to the right. Then the airspeed dropped from 144 kts to 121 kts. Applied power to pull up, and the missed approach was initiated. The aircraft kept descending to 60 ft above the ground before the pilot was able to stop the descent by using considerable power while pulling the nose up to an abnormally high angle. (From Exhibits 2-V and Flight Recorder.)

Aircraft "J" (DC-8): rain was heaviest between 6 to 3 miles final. The INS wind reading at 1,500 ft was 230° at 30 kts with 2° left drift. At about 2 miles final, the aircraft lost 25 kts indicated airspeed. The subsequent approach and landing were normal. (From Exhibit 2-V.)

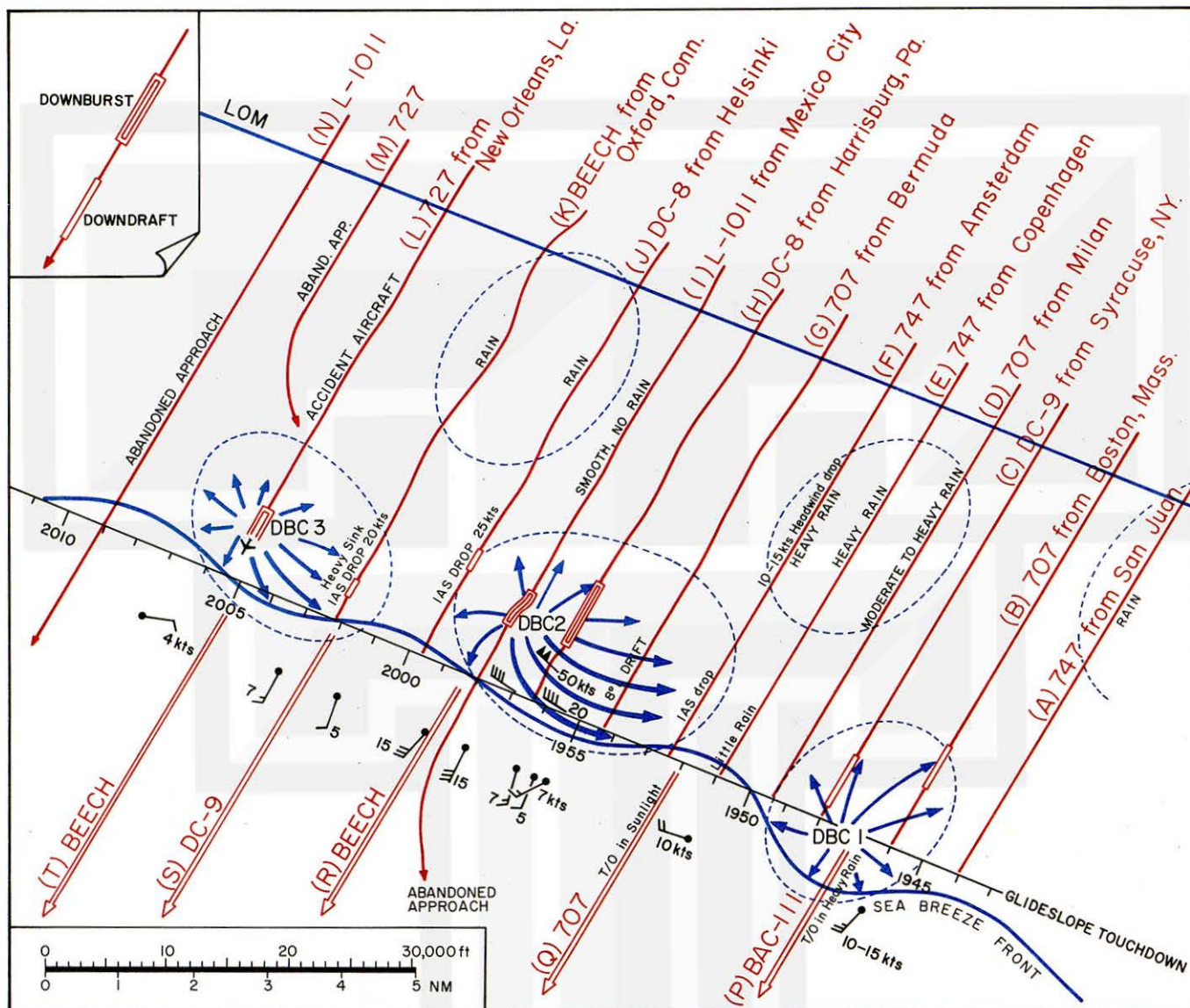
Aircraft "K" (Beech): encountered light turbulence and moderate to heavy rain from just outside the outer marker down halfway to middle marker. The approach continued normally until about 2 or 300 ft, where a heavy sink rate was experienced. The airspeed dropped about 20 kts. Applied power to recover from the sink; remainder of the approach was normal. (From Exhibit 2-V.)

Aircraft "L" (727): flew into rain at 700 ft. Rain became heavy at about 500 ft. The aircraft began sinking at 400 ft and airspeed dropped from 138 kts down to 122 kts in 7 seconds. The runway was in sight at 140 ft. The aircraft hit the approach lights at 2005+12 sec GMT about 2,400 ft short of the runway threshold. (From Flight Recorder and Exhibit 12-A.)

Aircraft "M" (727): following the previous aircraft on ILS approach. Instructed to go around at 2005+30 sec GMT. (From Exhibit 2-V and 3-C.)

The events experienced by Aircraft "A" through "M" were plotted on the time-space coordinates in an attempt to depict the meteorological conditions which had existed along the ILS approach path (Figure 25). The result revealed the existence of three major areas of localized outflow. There must have been a concentrated downward motion above each of these outflow areas. Without a massive supply of descending air, the intense outflow could not have originated nor been maintained.

The initial concept of a downdraft in a thunderstorm was introduced by Byers and Braham (1949) in their publication, "The Thunderstorm". The downdraft is a sustained, non-horizontal current of air descending in a thunderstorm. This current was identified as a downdraft provided the downward speed exceeded 3 fps. In order to distinguish an extremely intense downdraft from an ordinary one, Byers and Fujita (1975) introduced a new term, "DOWNBURST". A "downburst" is a localized, intense downdraft with vertical currents exceeding a downward speed of 12 fps or 720 feet per minute (fpm) at 300 ft above the surface. This value corresponds to a divergence of $4 \times 10^{-2} \text{ sec}^{-1}$.



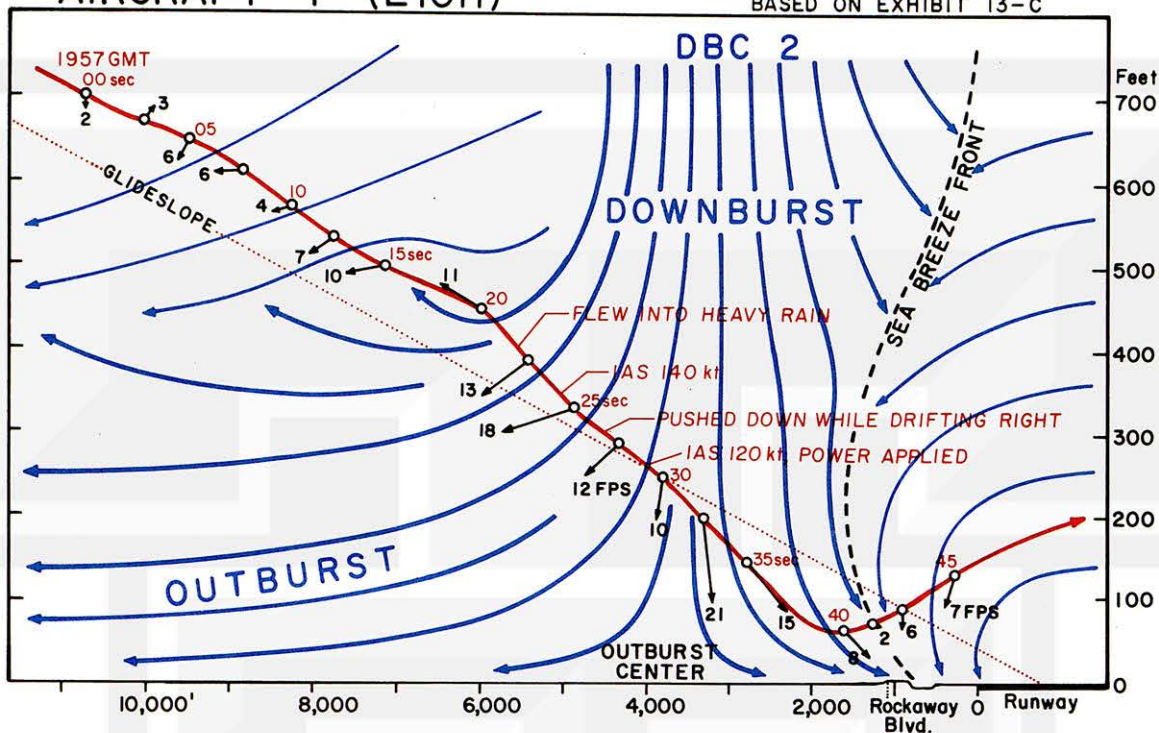
The paths of the approaching and departing aircraft drawn on time-space coordinates relative to the moving downburst cells near the threshold of runway 22-L at JFK Airport. Because of the sea-breeze front, the outburst air from these cells were held back to the north of the runway area (Top Figure of this page).

Shown on the opposite page are the paths of aircraft "I" and "L" in the vertical planes. The captain of Aircraft "I" executed the missed approach and applied power to approximately take-off range. The aircraft started recovering altitude at about 60 ft above the ground (Upper Figure).

Aircraft "L" was pushed down to the ground by an extraordinarily strong downburst (Lower Figure).

AIRCRAFT "I" (L1011)

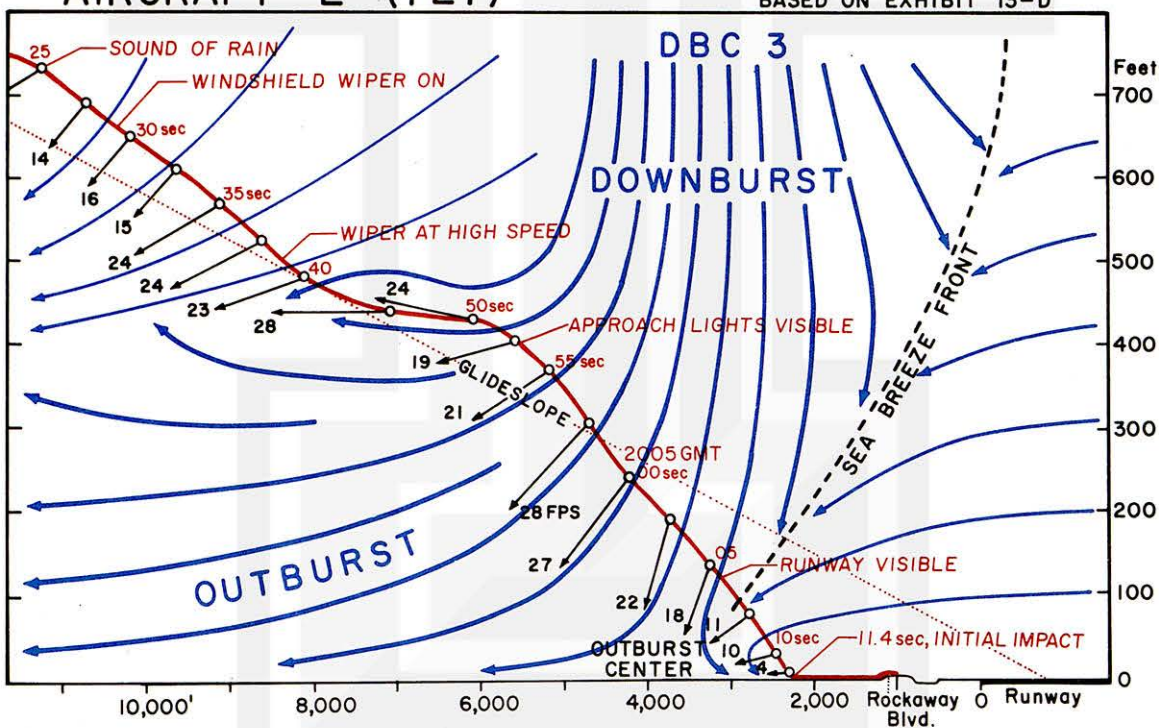
BASED ON EXHIBIT 13-C



33

AIRCRAFT "L" (727)

BASED ON EXHIBIT 13-D



37

The vertical rate of descent of an aircraft on a 3° glideslope in still air can be computed by $V \times \sin 3^\circ$. Representative rates computed by this equation are:

Airspeed	Rate of descent	
60 kts	5.3 fps	318 fpm
90	8.0	478
120	10.6	637
150	13.3	797
180	15.9	956

The velocities of the outflowing air from a downdraft or a downburst decrease with the distance from the cell. Therefore, if an aircraft was approaching a downburst cell (DBC), there might be no identifying drift, unusual rate of descent, or abnormal power requirement to alert the pilot, until after the effects of the downburst cell were encountered. Since an aircraft may fly into a downburst abruptly and unexpectedly, immediate recognition and quick action by the pilot would be necessary to overcome its effects. If the aircraft's position along the approach path did not provide sufficient time for pilot recognition and action, and aircraft response, the flight might not be able to execute a missed approach before contacting the ground.

Three downburst cells (DBCs) near the approach end of runway 22-L were identified as DBC 1, DBC 2, and DBC 3. Their widths were less than 3 miles and they were separated by relatively calm spaces between them (Figure 25).

Apparently the outflow from downburst areas did not move out into the runway area of JFK. None of the five aircraft, "P" through "T", encountered problems during their take-off from runway 22-R. The wind tower, located about one and a quarter mile southwest of the approach end of 22-L, was not affected by the outflow wind. The sea-breeze front lay between the wind tower and the approach path to runway 22-L.

The ground-level wind near the north boundary of the airport was entirely different from the reported winds. The captain of Aircraft "S", while taxiing on runway 31-L, observed small trees bending over from an estimated 20- to 30-mph wind blowing almost parallel to runway 13 - 31. Then he looked toward the approach end of 22-L to find Aircraft "H" getting in a nose-up attitude with its left wing down.

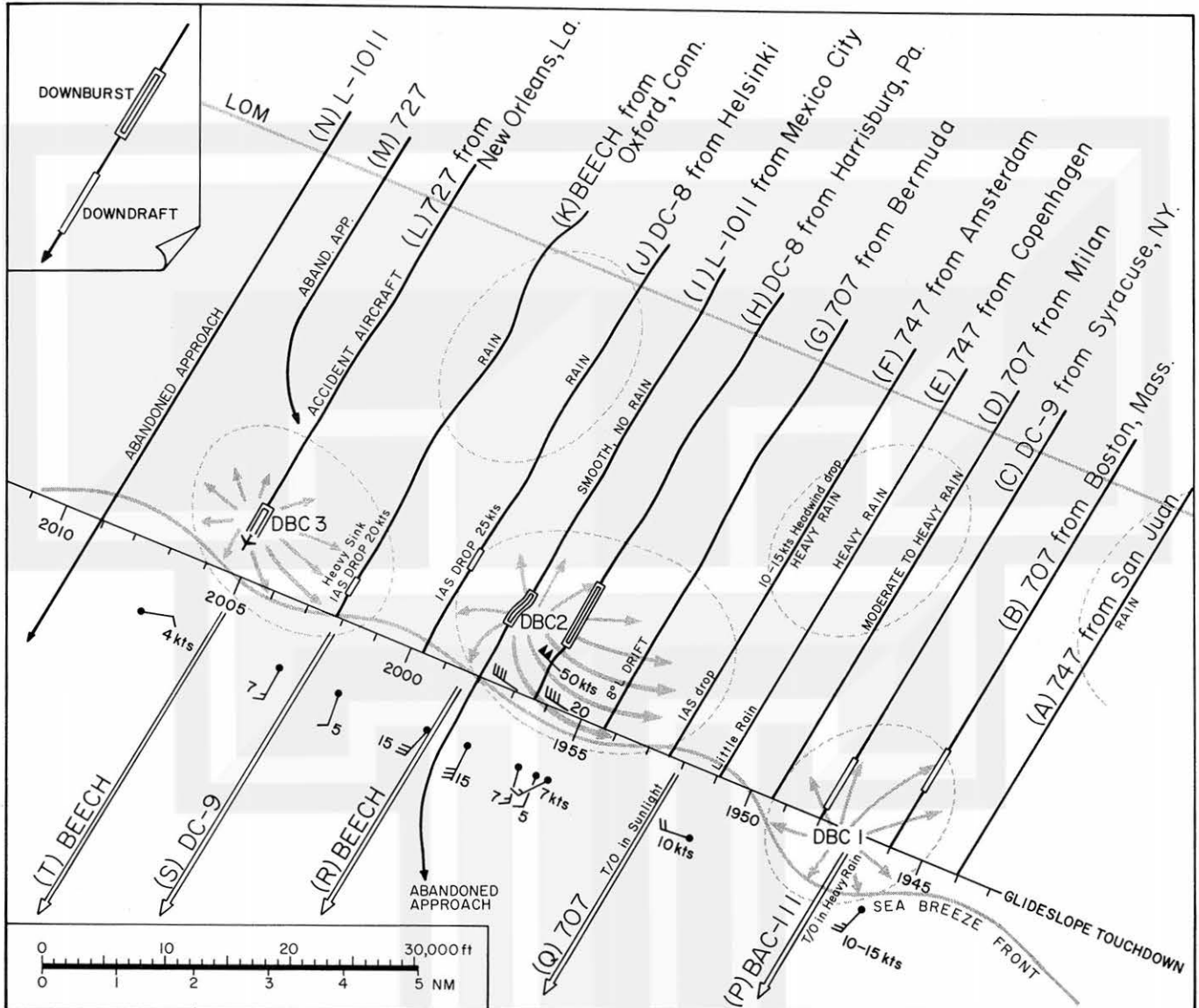


Figure 25. Three downburst cells (DBC) depicted on time-space coordinates. DBC 1 was on the runway threshold and DBC 2 affected seriously the approach effort of aircraft "H" and "I". DBC 3 blew aircraft "L" down to the ground, 2,000 ft short of runway 22-L. Most of the airport was under the influence of sea breeze. The outflow from downburst cells was distorted by the sea breeze front, resulting in the strong outflow winds to the north of the front.

However, the pilot was able to bring the aircraft to a more normal position before landing on 22-L.

The crosswind shear experienced by Aircraft "H" was spectacular. The 228° heading at 1955+58 sec was changed to 237° at 1956+04 sec. It is likely that the pilot responded to the sudden increase of crosswind from the right. The INS determined drift was 25° to 30° when IAS was 150 kts. A 60- to 70-kt crosswind would be required to produce such an extreme drift.

6. FLIGHT PATHS IN RELATION TO RADAR ECHOES

Excellent scope pictures at the WSR-57 radar of the National Weather Service at Atlantic City were taken every 5 to 6 minutes. The times of pictures taken shortly before the aircraft accident are

1945.7, 1951.4, 1956.7, and 2002.4 GMT.

Echoes in these pictures were contoured by their intensity. According to Gibson's (1975) interpretation, the three-level contours represent the theoretical rainfall rates, 0.1, 0.5, and 1.0 inch per hour. As estimated in Section 4, the height of the radar beam above the JFK area was about 7,000 ft. These rainfall rates, therefore, could be significantly different from those on the ground or along the ILS glideslope.

The three-level iso-echo contours at 1945.7 GMT were placed on a local map covering the JFK Airport and vicinity. The accident Aircraft "L" en route from New Orleans was in a holding pattern to the east of Asbury Park, N. J.

At this time, the spearhead echo which caused the 55-kt wind at the Morristown, N. J. Airport at 1915 GMT had already reached the JFK area. A weak downburst cell, DBC 1, was passing over the approach end of 22-L. Aircraft "P" took off from 22-R in heavy rain with windshield wipers on full speed. The rain ended when the aircraft was leaving the runway. Aircraft "B" and "C" were affected by the downburst DBC 1.

DBC 2 was moving toward JFK followed by DBC 3, which had crossed the East River over to northern Brooklyn. Apparently all three DBCs missed the four wind recorders in the New York City area. The peak wind speeds were recorded as follows:

Wind Recorder	Height above Grnd.	Time	Peak Wind	Closest DBC
LGA	20 ft	2011 GMT	18 kts	DBC 4 or 5
Central Park	132	1952	24	DBC 4
EWR	15	1937	32	DBC 3 or 4
JFK	20	1950	10	DBC 1
same	same	1956	17	DBC 2
same	same	2005	10	DBC 3
same	same	2020	14	DBC 4

Wind warnings for aviation interests are issued if winds are expected to equal or exceed 35 kts. None of these peak winds was fast enough to initiate a warning. An

irony of fate had permitted all of the four, or possibly five, DBCs to sneak through between the wind recorders. Had they approached from due west, the first one certainly would have been caught by EWR. An approach from the northwest would have provided a definite chance of detection by both Central Park and LGA.

The meteorological tower operated by the Long Island Lighting Company (LILCO) depicted the passage of the downburst cells. The instrumented tower, with an anemometer at a 205 ft level is located at Oceanside about 7 miles east-southeast of the accident site (Figure 26). The recorded winds plotted on a time-space diagram reveal the flow patterns of the weakening DBCs. The LILCO tower had been recording a 20-mph sea breeze prior to the onset of the downburst (Figure 27).

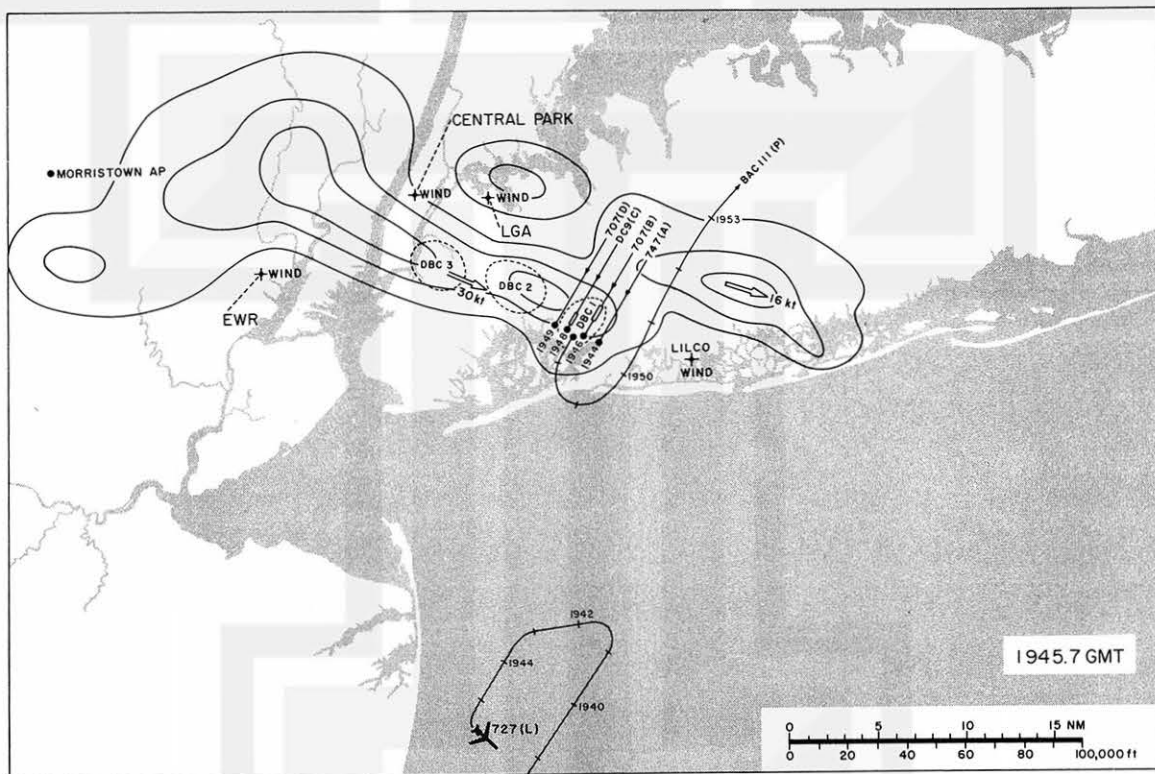


Figure 26. Radar echoes at 1945.7 GMT and the aircraft paths converted into time-space domain.

At 1951.4 GMT, the spearhead echo extended from lower Manhattan to the north of JFK. Aircraft "D" through "G" landed without incident. Accident Aircraft "L" headed toward the south coast of Long Island (Figure 28).

A helicopter en route from LGA to EWR encountered the fourth downburst cell, DBC 4. A thunderstorm with heavy rain was moving over the south half of

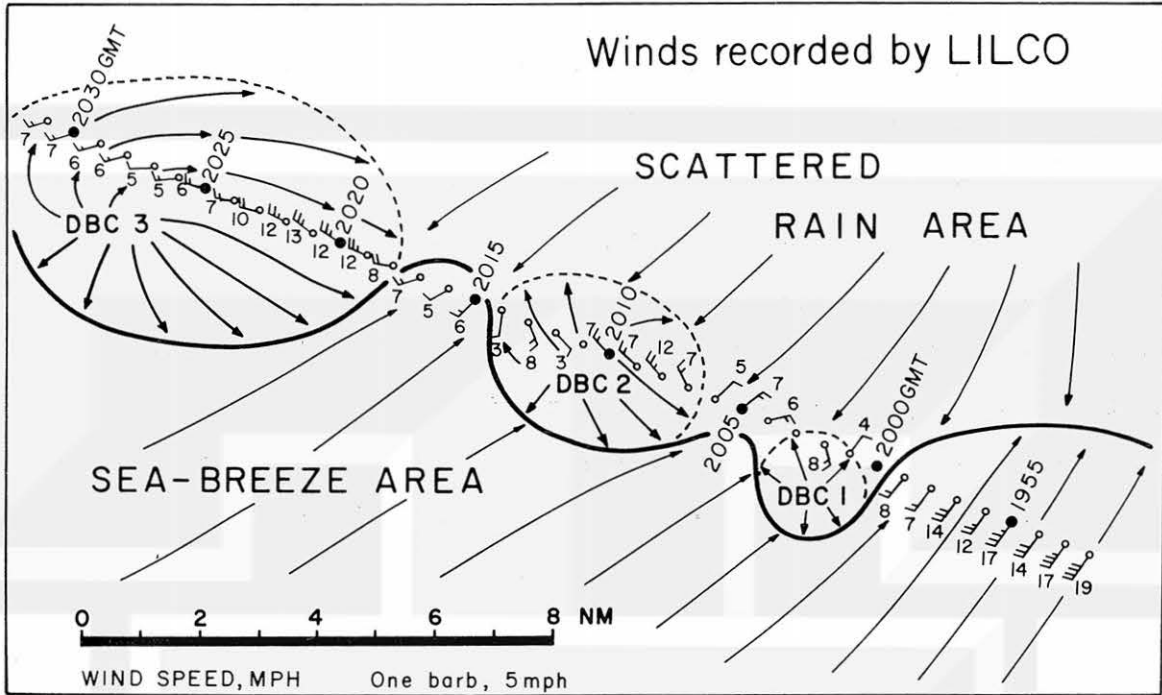


Figure 27. Depiction of three downburst cells by winds recorded by LILCO. 7 miles east-southeast of JFK Airport.

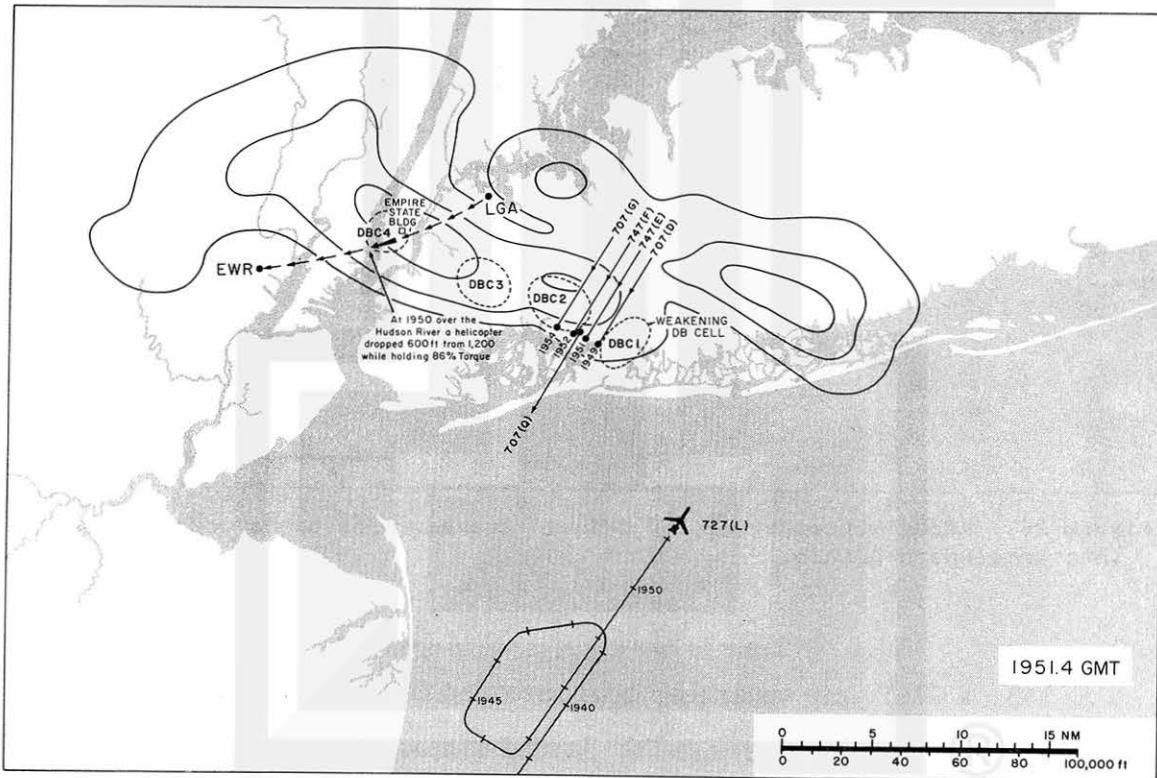


Figure 28. Four downburst cells in relation to the spearhead echo at 1951.4 GMT.

Manhattan and the upper New York Bay area. The helicopter flying at 1,200 ft passed just to the south of the Empire State Building, 1472-ft high including the TV antenna mast. At 1950 GMT, over the Hudson River, it flew into extremely heavy rain with drastically reduced visibility. On the west side of the river, the helicopter dropped to 600 ft while holding 86% torque, which is the maximum continuous power. The drop was due to the vertical current, which, while neither sharp nor sudden, was nevertheless very strong, requiring full continuous power just to maintain height after losing 600 ft. In the matter of a minute or so, it was in the clear and flew to Newark.

Before reaching the coast, Aircraft "L" descended from 7,000 to 4,000 ft. It then flew around a rain cell, crossing the shore line at 1955.6 GMT. At 1956.7 GMT, the radar time, Aircraft "L" was just to the northeast of the rain cell. Aircraft "H" landed after suffering from a severe crosswind shear and Aircraft "I" was approaching DBC 2 (Figure 29).

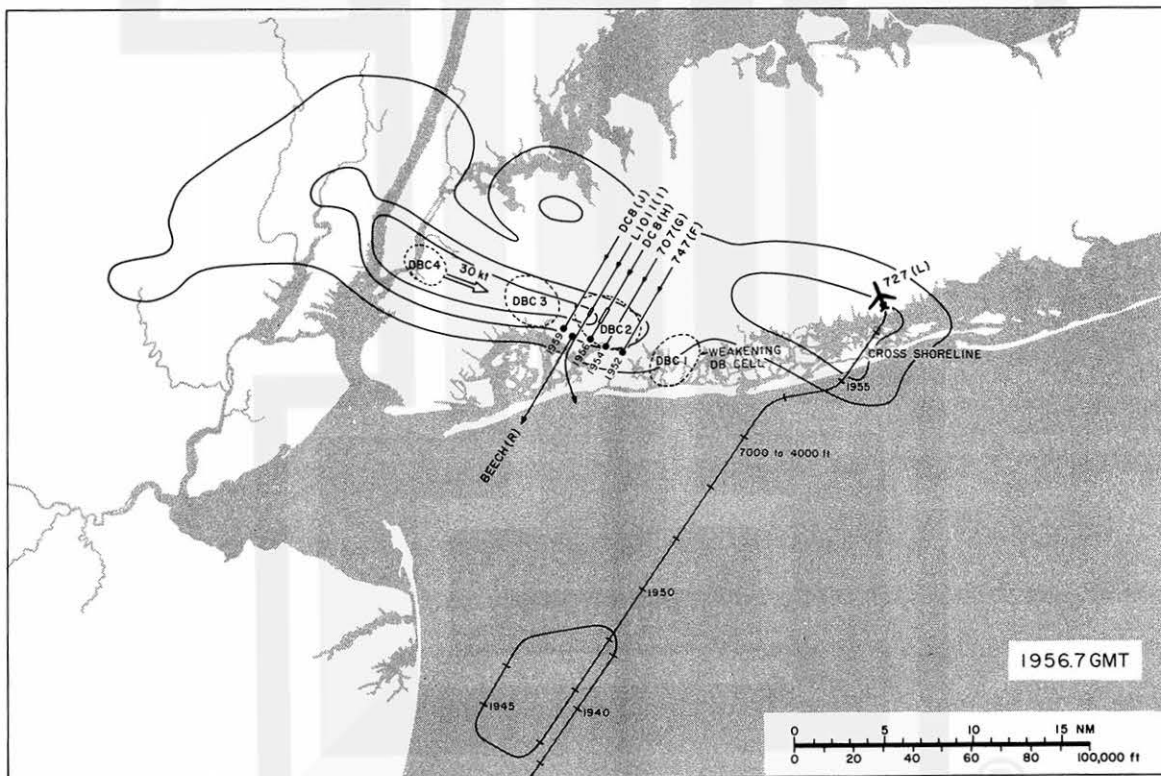


Figure 29. Radar echoes at 1956.7 GMT and aircraft paths converted into time-space domain.

At 2002.4 GMT, the next radar time, Aircraft "L" was approaching the outer marker with the landing gear down. A few minutes later, at 2006, Aircraft "N" observed on airborne radar a circular cell about 3 miles in diameter located over the threshold of runway 22-L. Aircraft "L" had hit the ground short of the runway (Figure 30).

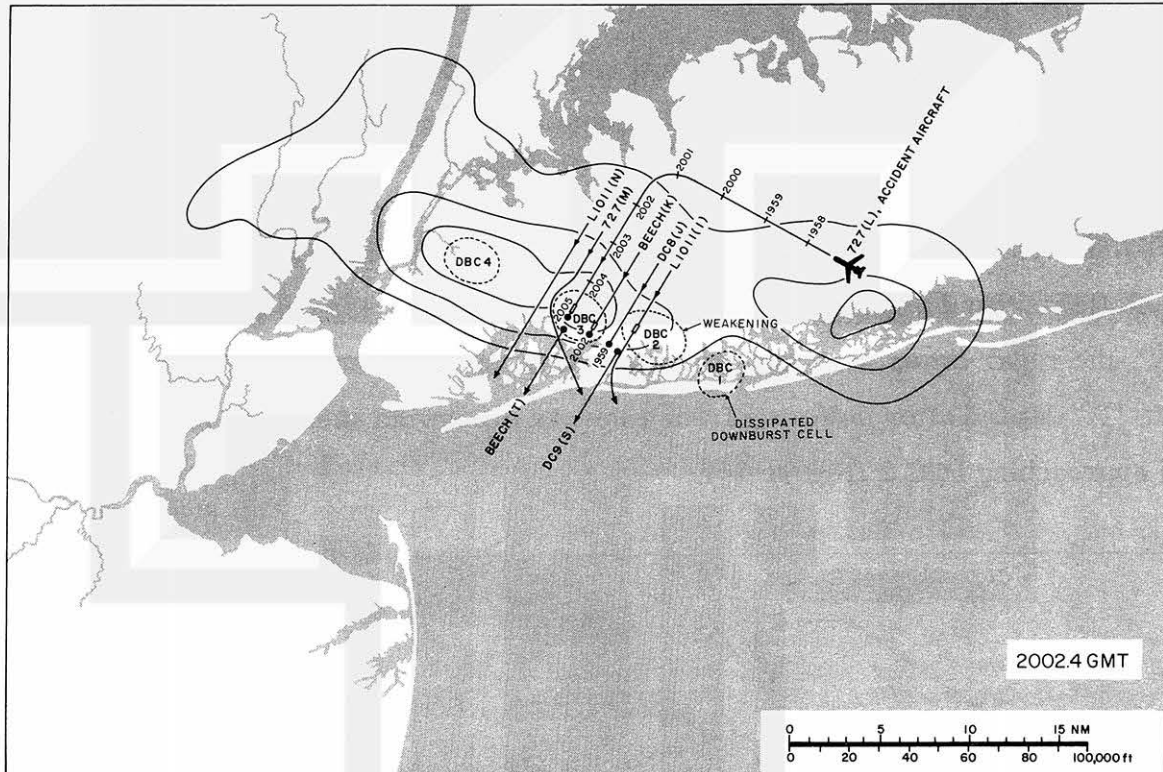


Figure 30. Radar echoes at 2002.4 GMT, just about 3 minutes before the accident.

7. EFFECTS OF DOWNBURST AND WIND SHEAR

Aircraft "I" (L-1011) initiated the missed approach after experiencing a heavy sink and right drift. The plane was obviously under the influence of a strong descending current and a crosswind from the left. The loss of indicated airspeed suggests a significant decrease in the headwind component.

In an attempt to reconstruct the pattern of airflow in the vertical plane, solutions of environmental winds in Exhibit 13-C and its supplement were examined. When the flow fields were delineated from these two solutions, the one in Exhibit 13-C appeared to be far more realistic from a meteorological point of view.

The headwind component in Exhibit 13-C shows that Aircraft "I" was experiencing about 15 fps (9 kts) headwind when it flew into heavy rain at about 400 ft. At 250 ft, the headwind changed into tailwind. Downward current then intensified reaching 21 fps at 210 ft (Figure 31).

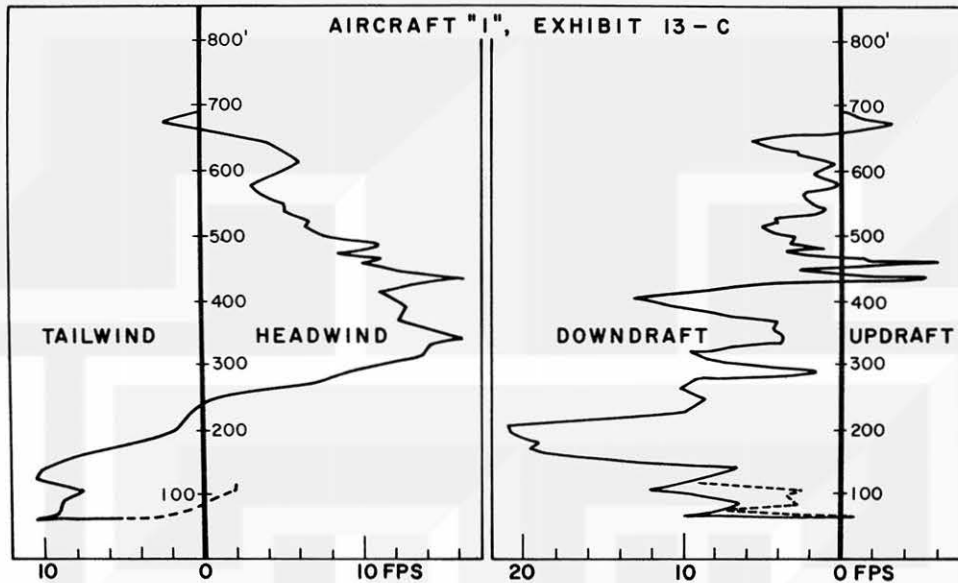


Figure 31. The wind profiles of Aircraft "I" from Exhibit 13-C. Winds are plotted as the function of height above runway.

"The Thunderstorm" (1949) revealed the frequency distribution of downdraft speeds measured at various altitudes during the 1946 and '47 seasons of Project operation in Florida and Ohio, respectively. According to the statistics, the mean downdraft values increase from theoretical "zero" at the surface to about 10 fps at the 4,000 ft level. The high values are approximately three times larger than the mean values at various altitudes (Figure 32). It is evident that the vertical speed of the downburst, 12 fps or larger at 300 ft above the ground, is about ten times larger than the mean downdraft speed estimated from "The Thunderstorm".

The effect of the downburst upon the maneuver of Aircraft "I" can be effectively shown on the height-distance diagram, which includes the flight path and the two-dimensional winds (Figure 33). The L-1011 (aircraft "I") was descending above the ILS glideslope until approximately 400 ft at which time it flew into heavy rain, with zero visibility. As the descent continued, the aircraft sank below the glideslope and was pushed to the right of the extended centerline of the runway. The

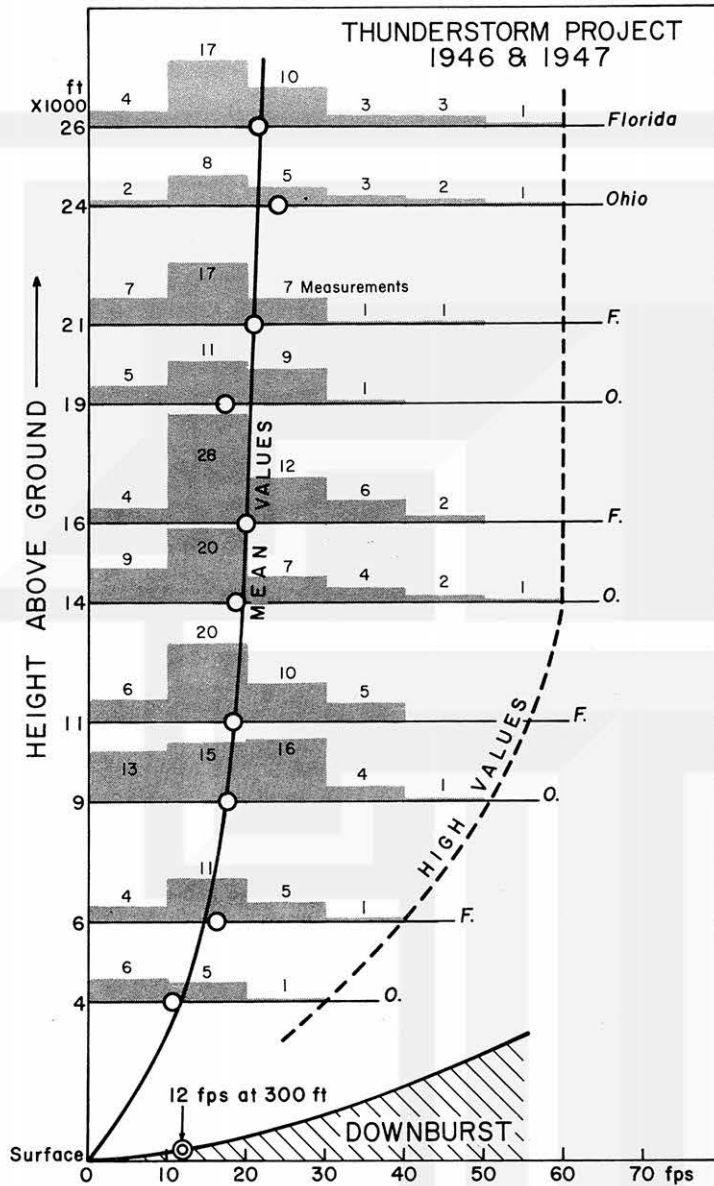


Figure 32. Frequencies of downdraft speeds measured by the Thunderstorm Project, 1946 and '47. Frequencies were plotted from Table 10 of the Thunderstorm (1949).

sinking motion and the right drift occurred simultaneously. The missed approach was executed and power was applied to approximately take-off range. The pilot was able to keep the wings level while involved with the low airspeed and high rate of descent. The aircraft continued sinking until it started recovering altitude at about 60 ft above the ground.

When the aircraft broke out into the clear, it was about halfway down the approach lights and to the right of the extended centerline of the runway. It continued on the missed approach procedures toward the runway heading. A few minutes later, the JFK Airport was closed due to the accident of Aircraft "L"; and the L-1011 diverted to EWR and landed without encountering any additional significant weather.

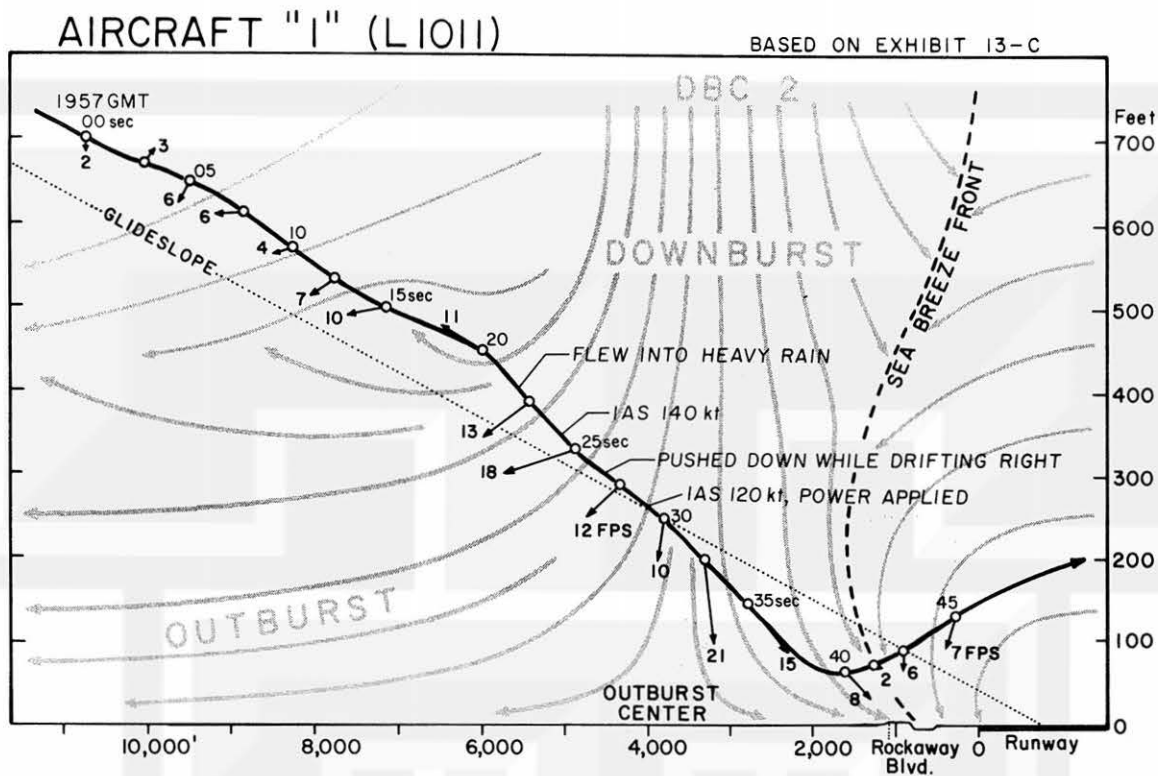


Figure 33. The path of Aircraft "I" through downburst cell No. 2.

In general, the air near the ground spreads out violently from the "outburst center", the spreading center above the ground. Unless a heading correction is made immediately, an aircraft in the crosswind burst will drift away from its expected course. If an aircraft flies straight into the outburst center, its indicated airspeed will increase momentarily followed by a high rate of sink. Before the aircraft can break out of the downburst cell, its indicated airspeed will drop suddenly, due to an increase in the tailwind component (Figure 34). The strong wind shear encountered by Aircraft "I" was the result of a downburst which produced vertical and horizontal shear. Any aircraft encountering such a downburst would lose altitude and/or drift to either the left or the right, depending on its position in relation to the center of the downburst.

"Wind Shear" is a very important phenomenon which could affect the aircraft during a final approach in various ways. This term, however, is used differently in aviation and in meteorology.

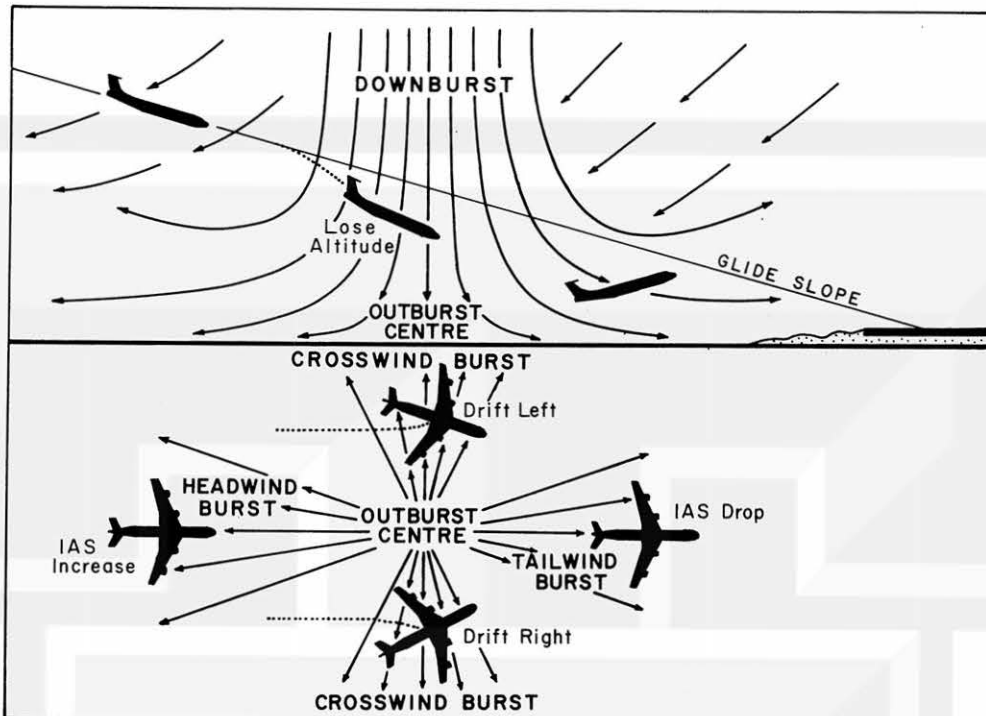


Figure 34. Effects of downburst and outburst upon aircraft during a final approach. Of these the most dangerous one is the downburst, crosswind burst, and tailwind burst encountered near the ground. Outburst is defined as being the strong outflow created when a downburst hits the ground and spreads out.

The meteorological definition of "wind shear" is the local variation of the wind vector or its components in a given direction and distance. The direction can be either horizontal or vertical, so that we may define

- a. vertical variation of horizontal winds
- b. horizontal variation of vertical winds.

These values can be expressed by the variation per distance, such as kt/mile, kt/1000 ft, m/sec per meter, etc.

In aviation the effect of the wind shear is felt as the time variation of winds rather than the spatial variation. Furthermore, the direction is taken along the flight path. An aircraft may experience difficulty when it encounters a sudden change in the wind, both in direction and speed. The vectorial difference of the wind between two points on the flight path is the vector shear, since

$$\text{Vector Wind Shear} = \frac{\text{Wind B minus Wind A}}{\text{Flight time between A and B}}$$

When the aircraft flies further, B to C, C to D, etc., the vector wind shear will vary successively (Figure 35).

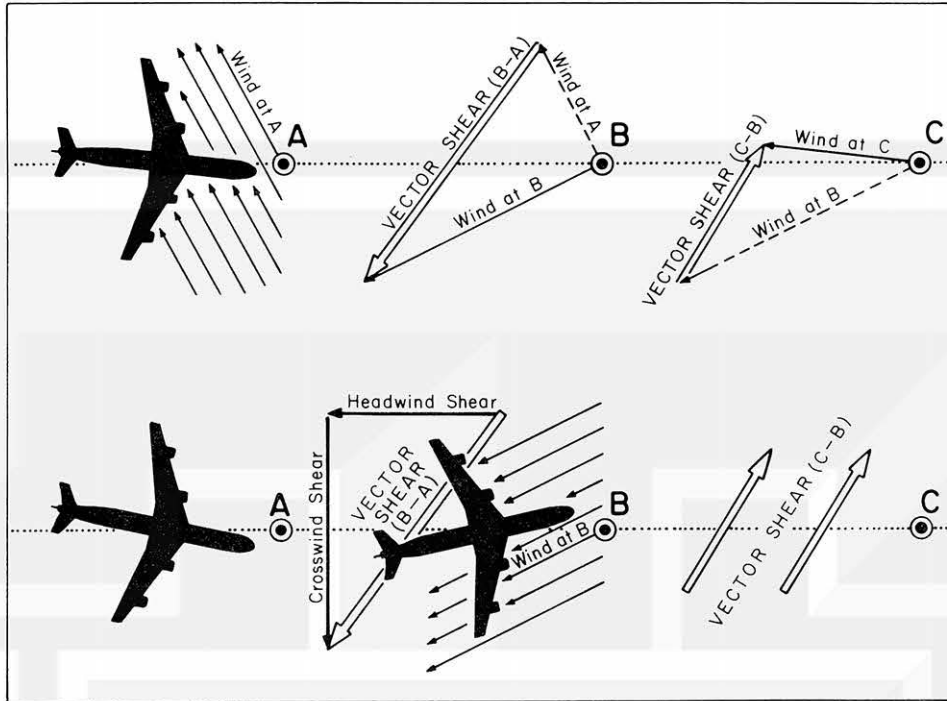


Figure 35. Pictorial expression of vector shear, headwind shear, and crosswind shear likely to be encountered by an aircraft flying in or near a downburst cell.

Two components of the vector wind shear are identified technically as "crosswind shear" and "head- or tailwind shear". This analysis considers the effects on an aircraft during an ILS approach wherein the aircraft must remain within close limits to the on-course of both the localizer and the glideslope signals. Such precision would not be required at a higher altitude.

Shear may affect an aircraft along any of its three axes. Shear causes action; pilots react; and the resulting corrections keep the aircraft on course. If the force of the shear exceeds the capability of the aircraft to maintain its desired path, it would experience excessive deviations. Wind shear may be severe enough to cause accelerations which a pilot can recognize as vestibular cues to a change in direction or velocity.

Crosswind Shear - A sudden change in wind direction and/or speed, such as a "crosswind burst", may carry the aircraft sideways, momentarily. This may be recognized by the pilot as a skid or a slip. These sensations are not common when flying heavy aircraft, and would be an alert cue to expect displacement from the localizer. Continuing the approach would require a sufficient altitude to permit a heading correction.

Headwind or Tailwind Shear - A sudden change in the headwind or tailwind does not affect drift, and heading corrections are not required. Since acceleration and deceleration are common sensations in flying, these cues would not alert a pilot. He could recognize head or tailwind shear by sudden changes in indicated airspeed.

Each aircraft has a speed associated to power vs. drag (speed stability). Rapid changes in the mass of air through which the aircraft is flying upset this relationship. Headwind shear would cause IAS to momentarily increase until the aircraft re-established its speed stability. It would be necessary for the pilot to lower the nose of the airplane and make a power reduction in order to remain on the glideslope. As the increased IAS dissipates, additional power would again be required as the ground speed would be decreasing and time-to-runway would increase.

Tailwind shear will cause IAS to decrease rapidly. Power must be increased simultaneously with the raising of the nose of the airplane in order to remain on the glideslope.

Vertical Wind Shear - Although in aviation, the variation in the up- or downdraft along the flight path is often called the "Vertical Wind Shear", this term in meteorology denotes the variation of horizontal wind along the vertical. Unless a spacecraft takes off or lands vertically, the vertical wind shear in the meteorological sense is not too important. In aviation, however, "Vertical Wind Shear" means the variation of vertical wind along the flight path. After an aircraft flies through a strong downward current, which does not vary horizontally, it could still be blown down toward the ground.

An aircraft flying into a vertical wind shear will momentarily accelerate in the vertical plane. This may be recognized by the pilot as a sinking sensation similar to an elevator descending. The pilot would have to bring the aircraft nose up and increase the power in order to maintain or regain the glideslope position. A strong or long-duration vertical wind shear would require an unusually high airplane body angle to create sufficient lift to maintain the glideslope position. A very high body angle would be necessary to stop the descent and to enable the airplane to execute a missed-approach.

The four most important winds and their effects may be identified as:

- (I) CROSSWIND SHEAR - Aircraft drifts to the right or left.
- (II) TAILWIND SHEAR - Indicated airspeed drops suddenly and aircraft sinks.
- (III) HEADWIND SHEAR - Indicated airspeed increases suddenly and aircraft gains altitude.
- (IV) DOWNBURST - Aircraft sinks abruptly.

Three wind profiles, A, B, and C of Aircraft "L" which were presented in Exhibit 13-D were examined. Of these, A had been computed by assuming that the approach power was a fuel flow of 4,596 lb/engine, a constant until descending to 140 ft. Thereafter, the power setting was 58%. In computing wind profile B, the engine thrust was varied between a few % to 47% in order to generate the actual sink rate under the assumption of no downdraft. Wind profile C was computed by assuming the horizontal wind profile B, and keeping the engine power constant at 4,596 lb/engine of fuel flow. Then the downdraft was computed in order to generate the actual sink rate.

From a meteorological point of view, wind profile A is more reasonable than B or C. Seen in profile A are the double maxima in downdraft speed at about 600 and 200 ft. The one at 220 ft reached 21 fps (1260 fpm), which would induce a 0.95 sec^{-1} or 340 hr^{-1} divergence below the flight altitude (Figure 36).

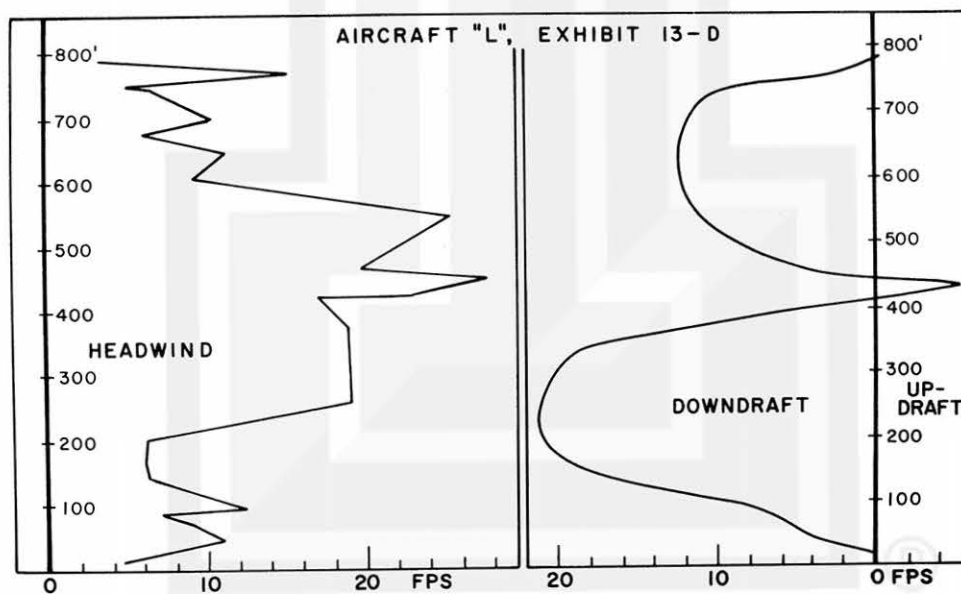


Figure 36. The wind profiles of Aircraft "L" from Exhibit 13-D. Winds are plotted as the function of height above the JFK runway level.

Aircraft "L" descended slightly above the glideslope in smooth air from the outer marker to 730 ft MSL where light rain was encountered. As it approached 500 ft, the windshield wipers were set at high speed, and the glideslope was intercepted. Exhibit 13-D (Figure 36) indicates two strong headwind gusts of 25 and 28 fps (15 and 17 kts) as it entered the downburst (Figure 37). The headwind decreased from 28 fps to 7 fps, while a 5 fps updraft changed to a 21 fps downburst. The loss of the headwind and the downburst which was encountered caused the aircraft to descend below the glideslope at 300 ft, near the core of the downburst.

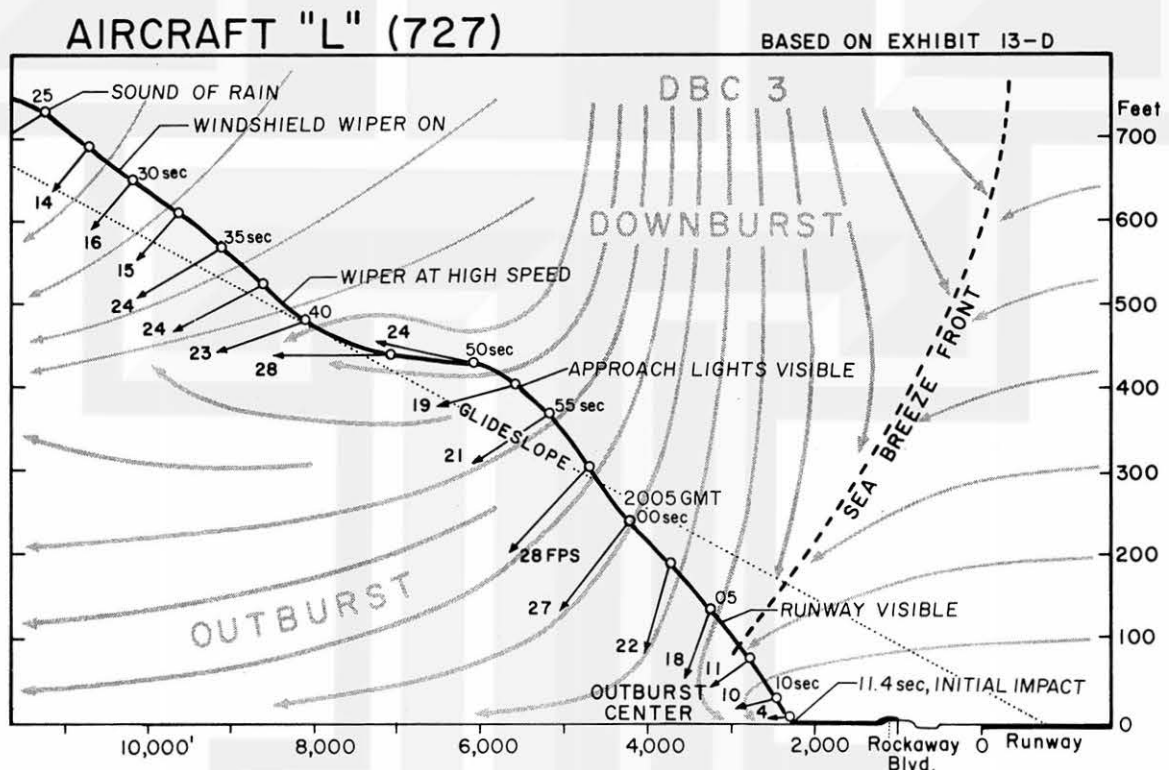


Figure 37. The path of Aircraft "L" through downburst cell No. 3 (DBC 3). The spreading beneath the cell was extraordinarily strong.

Until descending down to 130 ft the pilot of Aircraft "L" could not see the runway. He saw the JFK runway 22-L at 2005+06 sec GMT. About 5 sec later the initial impact took place. It is very difficult to determine the crosswind component during the final descent below 200 ft. The flight recorder data show that the heading changes were

Altitude (ft)	200	150	100	50	0
Heading	227°	226°	225°	227°	224°

The pattern of debris and the location of clipped approach lights suggests that, at the time of the impact, the aircraft was very slightly to the right of the approach center line, with the left wing down (Figure 38).

The author's initial attempt was to determine the surface wind based on the debris patterns. However, the distribution of debris seems to have been affected primarily by the aerodynamic forces acting upon the broken aircraft rather than by the wind near the ground. Moreover, the cushion effects of the air beneath the aircraft and the sloped edge of the landfill further complicate the final trajectories of all size pieces and debris.

It has been shown that the important winds affecting the aircraft during a final approach are tailwind or headwind shear, crosswind shear and downburst.

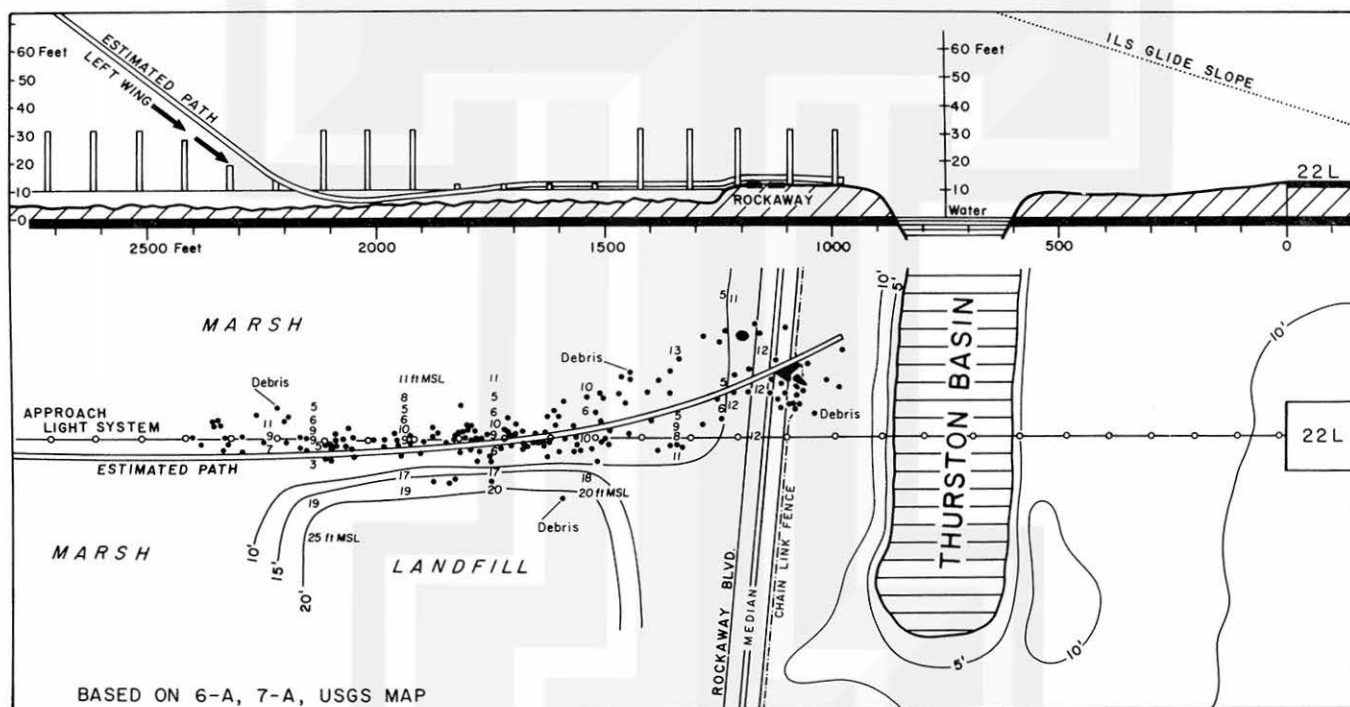


Figure 38. Distribution of the debris and the location of the approach lights from Exhibits 6-A and 7-A. The estimated path of the accident Aircraft "L" was drawn by the author in an attempt to determine the low-level winds from debris distribution. The path could be different from the ones determined by aeronautical methods after putting all debris together.

8. SPECULATION ON SPEARHEAD ECHOES

The downburst cells found inside the spearhead echo of the JFK Thunderstorm were different from most downdraft cells seen inside the ordinary thunderstorm. Namely, the downburst cells moved very fast while maintaining a very strong downward current near the surface.

According to "The Thunderstorm" (1949) most downdrafts originate at the height of the mid-troposphere. Dry air entrains into the downdraft from the side of the parent cloud (Figure 39).

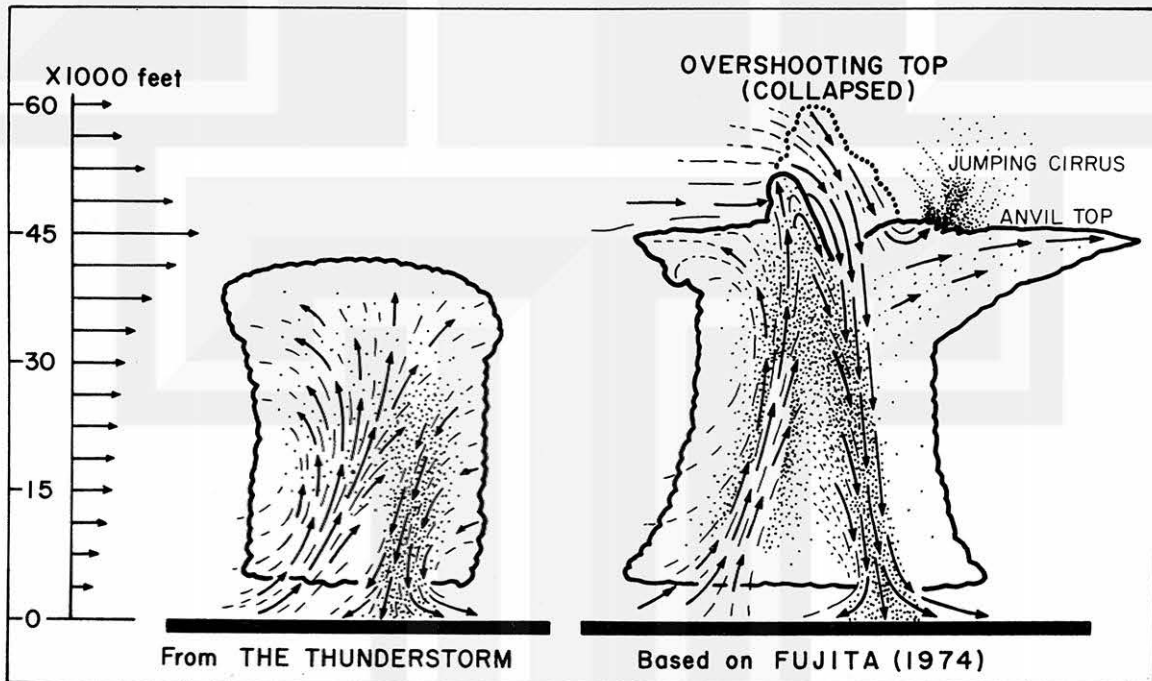


Figure 39. Models of thunderstorm circulation. Downdrafts in most thunderstorms originate in mid-troposphere (left). The stratospheric air above the anvil level plunges into the downburst.

In order to explain the intense vertical current and the fast-traveling speed of downburst cells, the author postulated a downburst cell originating in the lower-most stratosphere. The initial feature seen beyond the anvil-top level is the overshooting top which may reach 45,000 to 70,000 ft. When the top collapses, it undershoots into the anvil, transporting large horizontal momentum and dry air.

One of the greatest sinking velocities of the collapsing tops measured from a Learjet airplane by Fujita (1974) was 41 m/sec or 92 mph. It is hard to believe that there could be such a strong downward current at the anvil level (Figure 40).

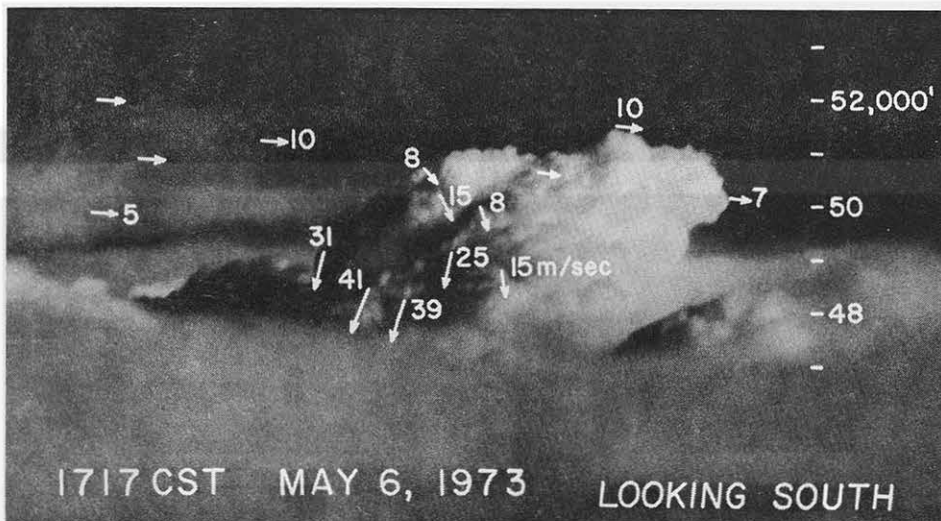


Figure 40. An extremely fast, descending motion atop a Texas thunderstorm of May 6, 1973. A downward velocity of 41 m/sec or 92 mph at 48,000 ft was measured by use of a picture sequence taken every second while flying at 45,000 ft in a research Learjet. By Fujita (1974).

When an overshooting top rises and then collapses rapidly, a downburst cell will form on the downwind side of the dome. The cell has a tendency to travel fast because it is fed by fast-moving stratospheric air. A successive rise and fall of the top will create a family of downburst cells which moves away from the parent thunderstorm (Figure 41).

On a PPI scope, the family of downburst cells might appear as a spearhead echo pointing downwind. From a close range, less than 30 miles, for instance, an airborne radar may be able to identify a downburst cell as being a circular area of rain. The pilot of Aircraft "M" observed a circular cell, 2 to 3 miles in diameter, located over the approach end of runway 22-L. The time of observation was 2006 GMT, when "M" was following the accident Aircraft "L".

During the damage survey of the April 3, 1974 tornado super-outbreak, the author witnessed from a low-flying Cessna airplane various patterns of tree damage. Some distance away from the tornado paths, trees in the forests were blown over in radial directions, as if they had been blown outward. It is suspected that these trees were pushed over or felled by strong winds which blew outward from the outburst center (Figure 42).

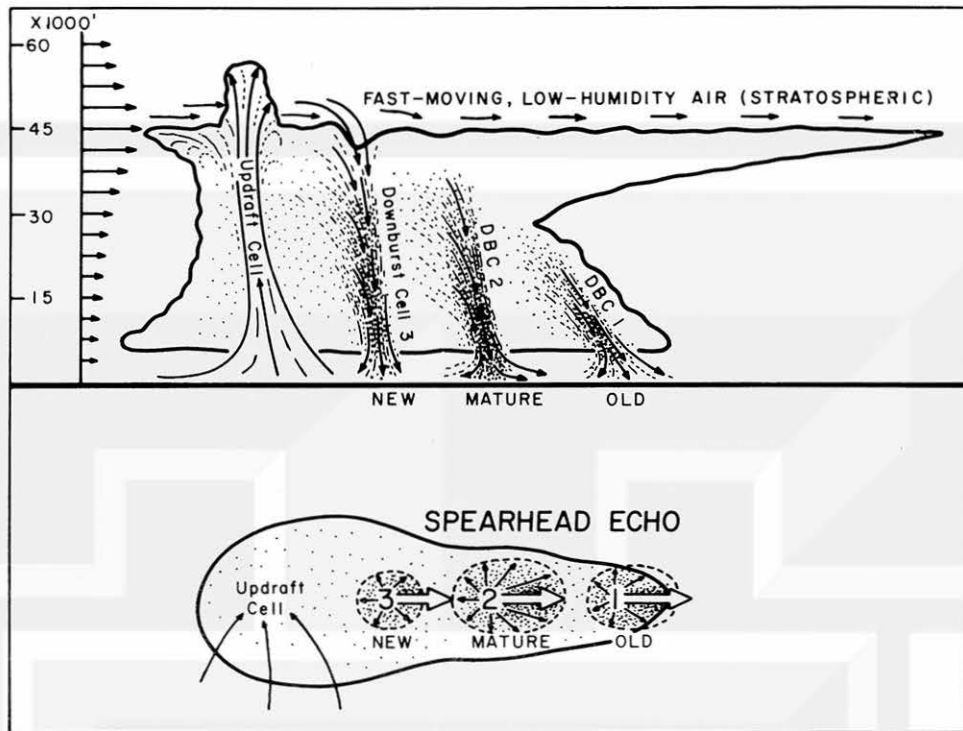


Figure 41. A model of spearhead echo. Being fed by the fast-moving, jet-stream air from above, downburst cells move faster than the parent cloud. A family of downburst cells in their various stages appears on radarscope as a spearhead-shaped echo. Low-humidity air is injected from the stratosphere, not from the side of the cloud.

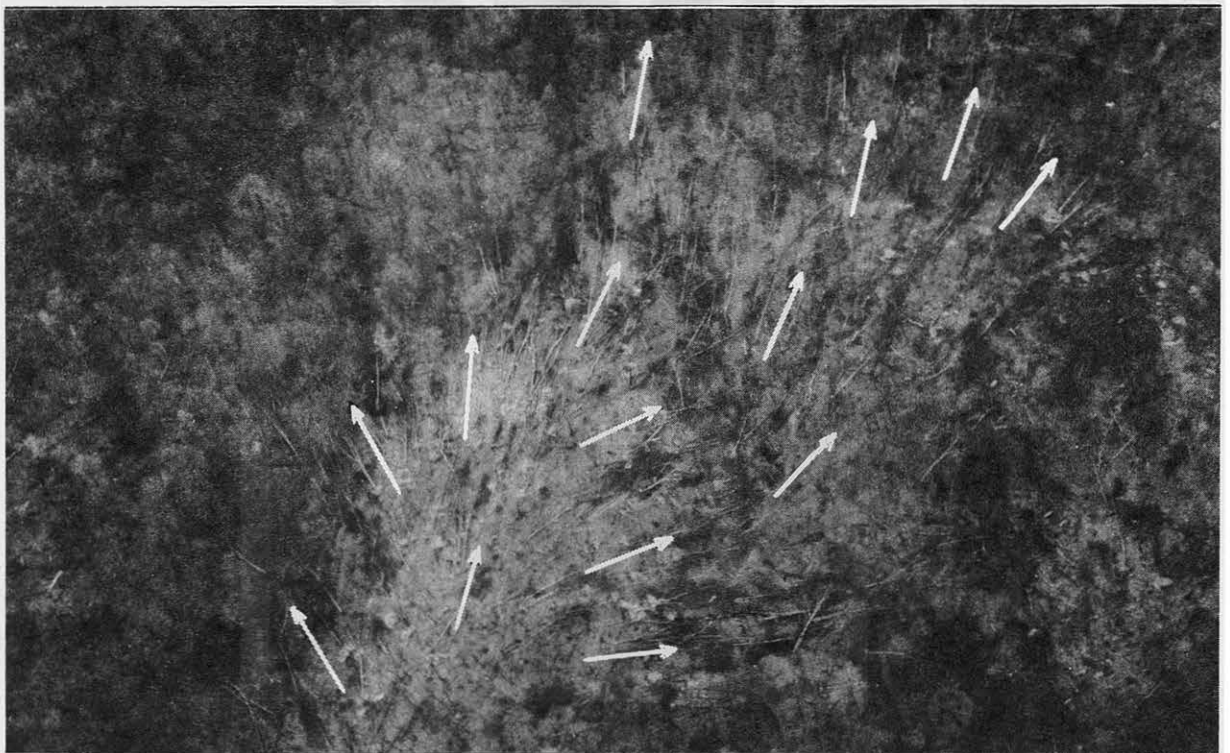


Figure 42. Over 300 trees blown over by an intense outburst near Beckley, West Virginia. Similar patterns of trees were photographed by the author at numerous locations along the paths of tornadic thunderstorms of April 3, 1974, the day of the super-outbreak tornadoes.

On May 6, 1975, the day of the Omaha tornado, WSR-57 radar of the National Weather Service at Kansas City, Missouri depicted a spearhead echo. The echo located approximately 100 nm south of the radar showed a feature of a spearhead pointing toward the east-southeast (Figure 43).

A geostationary satellite picture taken at 2222 GMT, the time of the radar picture shows an overshooting top. When the radar and satellite pictures were combined into a single image, it is evident that the overshooting top and the spearhead echo coincided very well in terms of their locations.

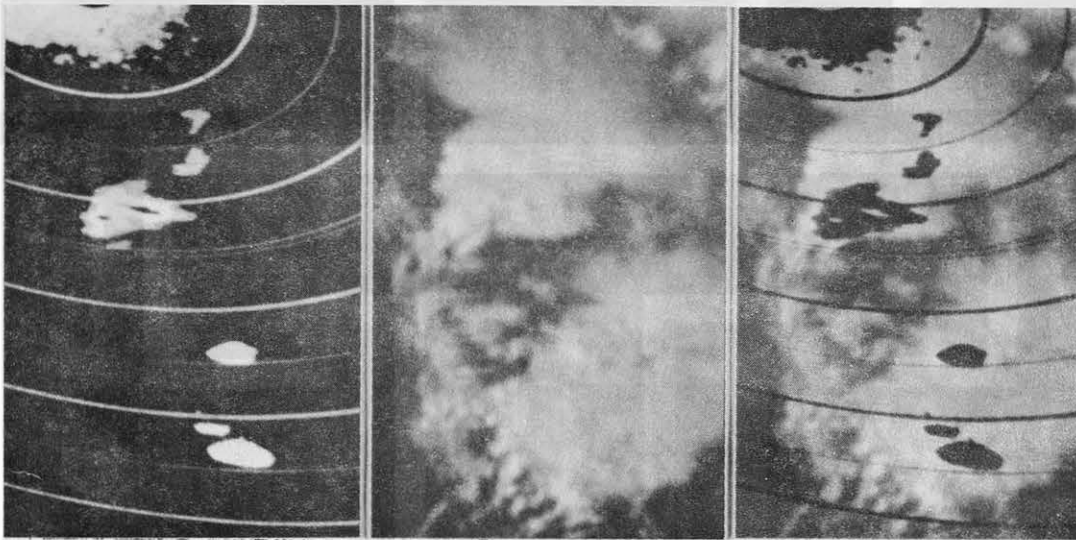


Figure 43. Features of a spearhead echo 100 nm to the south of Kansas City, Mo. on May 6, 1975. Radar echoes at 2222 GMT (left), SMS picture at 2222 GMT (center), and their combination.

9. CONCLUSIONS

The research results and the speculation regarding the phenomena presented in this paper suggest the existence of downburst cells in specific thunderstorms. These cells are likely to be characterized by spearhead echoes, a definition newly introduced in this paper. About 2% of the echoes in the New York area, the principal site involved in this research, were spearhead echoes.

The detection of downburst cells is very difficult because of their small sizes and short duration. Their existence might be identified by the following means.

1. Operate additional anemometers near the approach end of the active runway.
2. Both windspeed and directions must be monitored continuously during a thunderstorm, especially when a sea or lake breeze exists.
3. Continuously monitor the shape and motion of radar echoes. The development of monitoring techniques and display equipment is essential to adequately accomplish this.
4. The continuous monitoring of the cloud top activities. Development of a storm-detection satellite capable of watching cloud tops continuously, both day and night, by use of infrared and other sensors is recommended.

The detection and identification of any downburst cells that constitute a potential hazard to approaching and landing aircraft, will be of little use unless procedures are developed for the immediate communication of this information to the pilots of those aircraft. The rate of change of such cells would require their uninterrupted analysis, through the use of radar, mesometeorological analysis, surface wind information in the approach zone, etc., in order to properly evaluate the thunderstorm without unnecessarily disrupting the approach and landing of aircraft at a particular airport.

Once downburst cells are identified as being a potential hazard to approaching aircraft, the air traffic controllers, and the pilots, would have to take immediate action. The author is not qualified as an aviation authority, but suggests that the nature of downburst cells and the effects of wind shear would indicate the desirability of such action as:

1. Use of a runway which is not being affected by the downburst cell or the wind shear, if possible.
2. The air traffic controllers should advise a 2 to 3 minute delay in landing or takeoff when a strong cell is located near the approach or departure end.
3. The pilots of approaching aircraft should prepare to go around as soon as the effects of downburst and/or outburst is suspected.
4. A study should be made and the procedures tested for the proper control of the aircraft altitude to stop the sinking motion when a downburst is encountered.

Acknowledgements:

The author is very grateful to Captain L. Homer Mouden, Manager, Flight Safety, Eastern Airlines, and Mr. William R. Biggers, Director of Meteorology, Eastern Airlines, for their assistance in analyzing and interpreting the aircraft data. Sincere appreciation is due to Mr. Harold M. Gibson, Meteorologist-in-Charge, National Weather Service, New York City; Mr. Vincent J. Oliver, Chief, Applications Group, National Environmental Satellite Service; and Dr. William Nordberg, Director of Applications, National Aeronautics and Space Administration, for their suggestions and comments in performing meteorological aspects of this research.

Dr. Horace R. Byers, former Professor of Meteorology, The University of Chicago and Professor Emeritus, Texas A&M University, presently at Santa Barbara, California assisted the author in all aspects of this research. He directed the "Thunderstorm Project" in 1946 and '47, a joint project of four U. S. Government agencies: Air Force, Navy, National Advisory Committee for Aeronautics, and Weather Bureau.

It was at Dr. Byers' invitation that the author came from Japan in 1953 to conduct research under his direction at the University of Chicago. In understanding and solving complicated problems involved in this research, Dr. Byers provided very great assistance, leading to the introduction of several new terms. Without his personal interest and cooperation, this project could not have been accomplished.



REFERENCES

- Byers, Horace R. and Roscoe R. Braham, Jr. (1949): *The Thunderstorm*. Government Printing Office, Washington, D. C. 287 pp.
- Fujita, Tetsuya T. (1963): *Analytical Mesometeorology: A Review*. Meteorological Monographs, Vol. 5, No. 27, pp 77-125. American Meteorological Society, Boston.
- Fujita, T. Theodore (1974): *Overshooting Thunderheads Observed from ATS and Learjet*. SMRP Research Paper 117, 29 pp.
- Gibson, Harold M. (1975): *An Evaluation of Meteorological Conditions Near JFK International Airport on June 24, 1975*. NWSFO, New York City. 13 pp.
- National Transportation Safety Board Docket No. SA-451 --- Exhibits (1975)
- (2-A) Operations Group Chairman's Factual Report of Investigation.
 - (2-U) Statements of Witness Crewmembers. Aircraft "G" through "M".
 - (2-V) Statements of Crewmembers of Flights that Preceded or Followed Aircraft "L".
 - (3-C) FAA Transcripts, JFK Tower and NYCIFRR.
 - (6-A) Human Factors Group Chairman's Factual Report of Investigation.
 - (7-A) Structures Group Chairman's Factual Report of Investigation.
 - (12-A) Supplement to Specialist Factual Report of Investigation. Cockpit Voice Recorder, Aircraft "L".
 - (12-B) Cockpit Voice Recorder Group Chairman's Factual Report of Investigation, Aircraft "H".
 - (13-B) Position and Altitude Data Relating to the Final Approaches of Aircraft Inbound to JFK between 1950 and 2005 GMT.
 - (13-C) Data submitted by Lockheed California Company regarding the Analysis of DFDR Information from L-1011 Aircraft "I".
 - (13-D) Data submitted by the Boeing Company regarding the Analysis of FDR Information from 727 Aircraft "L".

GLOSSARY OF NEW TERMS

by

H. R. Byers and T. T. Fujita
November 1975

DOWNBURST - A localized, intense downdraft with vertical currents exceeding a downward speed of 12 fps or 720 fpm at 300 ft above the surface. This value corresponds to a divergence of $4 \times 10^{-2} \text{sec}^{-1}$.

SPEARHEAD ECHO - A radar echo with a pointed appendage extending toward the direction of the echo motion. The appendage moves much faster than the parent echo which is being drawn into the appendage. Downburst cells are most likely to be found in a spearhead echo.

WIND SHEAR - Meteorological definition is the spatial variation of the wind vector or its components in a given direction and distance. The direction can be either horizontal, vertical, or their combinations.

- a. Vertical variation of horizontal winds (vertical wind shear)
- b. Horizontal variation of vertical winds (shear in vertical velocity)
- c. Horizontal variation of horizontal winds (horizontal wind shear)

The term wind shear in aviation is the variation of the wind vector or its components along the flight path.

- a. Variation of crosswinds (crosswind shear)
- b. Variation of vertical winds (vertical wind shear)
- c. Variation of headwinds or tailwinds (headwind or tailwind shear)

OUTBURST CENTER - The nadir point of a downburst where the vertical air current hits the surface and spreads out violently. The fastest spreading flow is seen in the direction of the cell motion. Environmental flows, such as sea breeze and adjacent cells distort the outburst current. Depending upon the flight path relative to an outburst center, the outburst current is felt by an aircraft as

- a. Crosswind burst -- Aircraft drifts to the right or left.
- b. Tailwind burst -- Indicated airspeed drops and aircraft sinks.
- c. Headwind burst -- Indicated airspeed increases and aircraft gains altitude.

S U B J E C T I N D E X

Allentown Thunderstorm	18, 19	position at 1951 GMT	31
		position at 1956 GMT	32
Crosswind burst	37	position at 2002 GMT	33
		wind profile	36
Downburst		La Guardia Airport	
cells at LILCO	31	location in key map	9, 30
cells near 22-L	28, 29, 30, 31, 33	peak wind	29
definition	27	LILCO	
diagram	37	location	30
formation mechanism	43	wind	31
tree damage	44, 45	Mesoscale analysis	10, 11, 12, 13
Drift in crosswind burst		Morristown Municipal Airport	
aircraft G (707)	23, 28	55-kt wind	20, 29
aircraft H (DC-8)	23, 28	location in key map	9, 30
aircraft I (L-1011)	23, 28	Newark Airport	
Headwind burst	37, 40	location in key map	9, 30
		peak wind	29
Heavy sink in downburst		Outburst Center	37
aircraft H (DC-8)	23	Overshooting tops	43, 44
aircraft I (L-1011)	23, 34, 36	Sea Breeze Cumuli	10, 11
aircraft L (727)	24, 41	Spearhead echo	
helicopter	31, 32	Allentown Thunderstorm	18, 19
Hook echo	16	definition	17
I, aircraft		frequency	19
missed approach to 22-L	33	formation mechanism	43, 45
wind profile	34	JFK Thunderstorm	17, 19
JFK Airport		model cloud	45
location in key map	9	in Kansas	46
location in SMS image	2	Tailwind burst	37
peak wind	29	Thunderstorm Project	
JFK Thunderstorm		definition of downdraft	24
anvil height	2	downdraft frequency	34, 35
echo at 1753 GMT	10	Time-space coordinates	21, 22, 28
echo at 1851 GMT	11	Wind Shear	
echo at 2002 GMT	11	crosswind shear	37, 38, 40
echo at 2053 GMT	12	headwind shear	37, 39, 40
echo-top heights	14	meteorological definition	37
growth rate of cloud	8	tailwind shear	39, 40
infrared SMS images	4, 5, 6, 7	vector wind shear	37, 38
radar echo area	8	vertical wind shear	39
spearhead echo	16, 17, 18, 19		
visible SMS image	2		
L, aircraft			
heading below 200'	41		
impact area	42		
position at 1945 GMT	30		

MESOMETEOROLOGY PROJECT - - - RESEARCH PAPERS

(Continued from front cover)

42. A Study of Factors Contributing to Dissipation of Energy in a Developing Cumulonimbus - Rodger A. Brown and Tetsuya Fujita
43. A Program for Computer Gridding of Satellite Photographs for Mesoscale Research - William D. Bonner
44. Comparison of Grassland Surface Temperatures Measured by TIROS VII and Airborne Radiometers under Clear Sky and Cirriform Cloud Conditions - Ronald M. Reap
45. Death Valley Temperature Analysis Utilizing Nimbus I Infrared Data and Ground-Based Measurements - Ronald M. Reap and Tetsuya Fujita
46. On the "Thunderstorm-High Controversy" - Rodger A. Brown
47. Application of Precise Fujita Method on Nimbus I Photo Gridding - Lt. Cmd. Ruben Nasta
48. A Proposed Method of Estimating Cloud-top Temperature, Cloud Cover, and Emissivity and Whiteness of Clouds from Short- and Long-wave Radiation Data Obtained by TIROS Scanning Radiometers - T. Fujita and H. Grandoso
49. Aerial Survey of the Palm Sunday Tornadoes of April 11, 1965 - Tetsuya Fujita
50. Early Stage of Tornado Development as Revealed by Satellite Photographs - Tetsuya Fujita
51. Features and Motions of Radar Echoes on Palm Sunday, 1965 - D. L. Bradbury and T. Fujita
52. Stability and Differential Advection Associated with Tornado Development - Tetsuya Fujita and Dorothy L. Bradbury
53. Estimated Wind Speeds of the Palm Sunday Tornadoes - Tetsuya Fujita
54. On the Determination of Exchange Coefficients: Part II - Rotating and Nonrotating Convective Currents - Rodger A. Brown
55. Satellite Meteorological Study of Evaporation and Cloud Formation over the Western Pacific under the Influence of the Winter Monsoon - K. Tsuchiya and T. Fujita
56. A Proposed Mechanism of Snowstorm Mesojet over Japan under the Influence of the Winter Monsoon - T. Fujita and K. Tsuchiya
57. Some Effects of Lake Michigan upon Squall Lines and Summertime Convection - Walter A. Lyons
58. Angular Dependence of Reflection from Stratiform Clouds as Measured by TIROS IV Scanning Radiometers - A. Rabbe
59. Use of Wet-beam Doppler Winds in the Determination of the Vertical Velocity of Raindrops inside Hurricane Rainbands - T. Fujita, P. Black and A. Loesch
60. A Model of Typhoons Accompanied by Inner and Outer Rainbands - Tetsuya Fujita, Tatsuo Izawa, Kazuo Watanabe and Ichiro Imai
61. Three-Dimensional Growth Characteristics of an Orographic Thunderstorm System - Rodger A. Brown
62. Split of a Thunderstorm into Anticyclonic and Cyclonic Storms and their Motion as Determined from Numerical Model Experiments - Tetsuya Fujita and Hector Grandoso
63. Preliminary Investigation of Peripheral Subsidence Associated with Hurricane Outflow - Ronald M. Reap
64. The Time Change of Cloud Features in Hurricane Anna, 1961, from the Easterly Wave Stage to Hurricane Dissipation - James E. Arnold
65. Easterly Wave Activity over Africa and in the Atlantic with a Note on the Intertropical Convergence Zone during Early July 1961 - James E. Arnold
66. Mesoscale Motions in Oceanic Stratus as Revealed by Satellite Data - Walter A. Lyons and Tetsuya Fujita
67. Mesoscale Aspects of Orographic Influences on Flow and Precipitation Patterns - Tetsuya Fujita
68. A Mesometeorological Study of a Subtropical Mesocyclone -Hidetoshi Arakawa, Kazuo Watanabe, Kiyoshi Tsuchiya and Tetsuya Fujita
69. Estimation of Tornado Wind Speed from Characteristic Ground Marks - Tetsuya Fujita, Dorothy L. Bradbury and Peter G. Black
70. Computation of Height and Velocity of Clouds from Dual, Whole-Sky, Time-Lapse Picture Sequences - Dorothy L. Bradbury and Tetsuya Fujita
71. A Study of Mesoscale Cloud Motions Computed from ATS-I and Terrestrial Photographs - Tetsuya Fujita, Dorothy L. Bradbury, Clifford Murino and Louis Hull
72. Aerial Measurement of Radiation Temperatures over Mt. Fuji and Tokyo Areas and Their Application to the Determination of Ground- and Water-Surface Temperatures - Tetsuya Fujita, Gisela Baralt and Kiyoshi Tsuchiya
73. Angular Dependence of Reflected Solar Radiation from Sahara Measured by TIROS VII in a Torquing Maneuver - Rene Mendez.
74. The Control of Summertime Cumuli and Thunderstorms by Lake Michigan During Non-Lake Breeze Conditions - Walter A. Lyons and John W. Wilson
75. Heavy Snow in the Chicago Area as Revealed by Satellite Pictures - James Bunting and Donna Lamb
76. A Model of Typhoons with Outflow and Subsidence Layers - Tatsuo Izawa
77. Yaw Corrections for Accurate Gridding of Nimbus HRIR Data - R. A. Madden
78. Formation and Structure of Equatorial Anticyclones caused by Large-Scale Cross Equatorial Flows determined by ATS I Photographs - T. T. Fujita, K. Watanabe and T. Izawa
79. Determination of Mass Outflow from a Thunderstorm Complex using ATS III Pictures - T. T. Fujita and D. L. Bradbury
80. Development of a Dry Line as shown by ATS Cloud Photography and verified by Radar and Conventional Aerological Data - D. L. Bradbury
81. Dynamical Analysis of Outflow from Tornado-Producing Thunderstorms as revealed by ATS III Pictures - K. Ninomiya
- *82. Computation of Cloud Heights from Shadow Positions through Single Image Photogrammetry of Apollo Pictures - T. T. Fujita
83. Aircraft, Spacecraft, Satellite and Radar Observations of Hurricane Gladys, 1968 - R. C. Gentry, T. Fujita and R. C. Sheets
84. Basic Problems on Cloud Identification related to the design of SMS-GOES Spin Scan Radiometers - T. T. Fujita
85. Mesoscale Modification of Synoptic Situations over the Area of Thunderstorms' Development as revealed by ATS III and Aerological Data - K. Ninomiya
86. Palm Sunday Tornadoes of April 11, 1965 - T. T. Fujita, D. L. Bradbury and C. F. Van Thullenar
(Reprinted from Mon. Wea. Rev., 98, 29-69, 1970)

SATELLITE AND MESOMETEOROLOGY RESEARCH PROJECT --- PAPERS

87. Patterns of Equivalent Blackbody Temperature and Reflectance of Model Clouds computed by changing Radiometer's Field of View - J. J. Tecson
88. Lubbock Tornadoes of 11 May 1970 - T. T. Fujita
89. Estimate of Areal Probability of Tornadoes from Inflationary Reporting of their Frequencies - T. T. Fujita
90. Application of ATS III Photographs for determination of Dust and Cloud Velocities over Northern Tropical Atlantic - T. T. Fujita
91. A Proposed Characterization of Tornadoes and Hurricanes by Area and Intensity - T. T. Fujita
92. Estimate of Maximum Wind Speeds of Tornadoes in Three Northwestern States - T. T. Fujita
93. In- and Outflow Field of Hurricane Debbie as revealed by Echo and Cloud Velocities from Airborne Radar and ATS-III Pictures - T. T. Fujita and P. G. Black (Reprinted from Preprint of Radar Meteorology Conference, Nov. 17-20, 1970, Tucson, Arizona)
94. Characterization of 1965 Tornadoes by their Area and Intensity - J. J. Tecson
- *95. Computation of Height and Velocity of Clouds over Barbados from a Whole-Sky Camera Network - R. D. Lyons
96. The Filling over Land of Hurricane Camille, August 17-18, 1969 - D. L. Bradbury
97. Tornado Occurrences related to Overshooting Cloud-Top Heights as determined from ATS Pictures - T. T. Fujita
98. FPP Tornado Scale and its Applications - T. T. Fujita and A. D. Pearson
99. Preliminary Results of Tornado Watch Experiment 1971 - T. T. Fujita, J. J. Tecson and L. A. Schaal
100. F-Scale Classification of 1971 Tornadoes - T. T. Fujita
101. Typhoon-Associated Tornadoes in Japan and new evidence of Suction Vortices in a Tornado near Tokyo - T. T. Fujita
102. Proposed Mechanism of Suction Spots accompanied by Tornadoes - T. T. Fujita
103. A Climatological Study of Cloud Formation over the Atlantic during Winter Monsoon - H. Shitara
- **104. Statistical Analysis of 1971 Tornadoes - E. W. Pearl
105. Estimate of Maximum Windspeeds of Tornadoes in Southernmost Rockies - T. T. Fujita
106. Use of ATS Pictures in Hurricane Modification - T. T. Fujita
107. Mesoscale Analysis of Tropical Latin America - T. T. Fujita
108. Tornadoes Around The World - T. T. Fujita (Reprinted from *Weatherwise*, 26, No. 2, April 1973)
109. A Study of Satellite-Observed Cloud Patterns of Tropical Cyclones - E. E. Balogun
110. METRACOM System of Cloud-Velocity determination from Geostationary Satellite Pictures - Y. M. Chang, J. J. Tecson and T. T. Fujita
111. Proposed Mechanism of Tornado Formation from Rotating Thunderstorm - T. T. Fujita
112. Joliet Tornado of April 6, 1972 - E. W. Pearl
113. Results of FPP Classification of 1971 and 1972 Tornadoes - T. T. Fujita and A. D. Pearson
114. Satellite-Tracked Cumulus Velocities - T. T. Fujita, E. W. Pearl and W. E. Shenk
115. General and Local Circulation of Mantle and Atmosphere toward Prediction of Earthquakes and Tornadoes - T. T. Fujita and K. Fujita
116. Cloud Motion Field of Hurricane Ginger during the Seeding Period as determined by the METRACOM System - J. J. Tecson, Y. M. Chang and T. T. Fujita
117. Overshooting Thunderheads observed from ATS and Learjet - T. T. Fujita
118. Thermal and Dynamical Features of a Thunderstorm with a Tilted Axis of Rotation - T. T. Fujita
119. Characteristics of Anvil-Top Associated with the Poplar Bluff Tornado of May 7, 1973 - E. W. Pearl
120. Jumbo Tornado Outbreak of 3 April 1974 - T. T. Fujita
121. Cloud Velocities Over The North Atlantic Computed From ATS Picture Sequences - Y. M. Chang and J. J. Tecson
122. Analysis of Anvil Growth for ATS Pictures - Y. M. Chang
- *123. Evaluation of Tornado Risk Based on F-Scale Distribution - E. W. Pearl
124. Superoutbreak Tornadoes Of April 3, 1974 As Seen In ATS Pictures - T. T. Fujita and G. S. Forbes
125. Kinematic Analysis of Tropical Storm Based On ATS Cloud Motions - J. J. Tecson and T. T. Fujita
126. Overshooting Top Behavior of Three Tornado-Producing Thunderstorms - T. A. Umenhofer
127. New Evidence from April 3-4, 1974 Tornadoes - T. T. Fujita
128. Long-Term Fluctuation of Tornado Activities - T. T. Fujita, A. Pearson and D. M. Ludlum
129. Relationship between Tornadoes and Hook Echoes on April 3, 1974 - G. S. Forbes
130. Cloud-Top Parameters - A Hail Indicator - E. W. Pearl, W. E. Shenk and W. Skillman
131. Detection of Severe Storms by Satellites - T. T. Fujita
- *132. The Gothenburg Tornado Family of June 18, 1975 - G. S. Forbes
133. Analysis and Use of Meteorological Data: An Outline prepared for UN/WMO Regional Training Seminar (Nairobi) - T. T. Fujita
134. A Profile of an Easterly Wave from SMS Photographs and GATE Ship Reports - J. J. Tecson and E. E. Balogun,
135. Description of Mesoscale Systems - E. W. Pearl.
136. Cloud-Motion Vectors over the GATE area computed by McIDAS and METRACOM Methods - J. J. Tecson.

